THE INSTITUTE OF PAPER CHEMISTRY

Appleton, Wisconsin

BEHAVIOR OF FIBROUS AND NONFIBROUS COMPONENTS IN THE CORRUGATING OPERATION

PART I. ANALYSIS OF STRESS AND STRAIN IN MEDIUM DURING FORMATION OF THE FLUTES

Project 1108-22

Progress Report One

to

FOURDRINIER KRAFT BOARD INSTITUTE, INC.

February 29, 1960

TABLE OF CONTENTS

THE INSTITUTE OF PAPER CHEMISTRY

Appleton, Wisconsin

BEHAVIOR OF FIBROUS AND NONFIBROUS COMPONENTS IN THE CORRUGATING OPERATION

PART I. ANALYSIS OF STRESS AND STRAIN IN MEDIUM DURING FORMATION OF THE FLUTES

SUMMARY

A fundamental study of the stress-strain behavior of a medium during corrugating was undertaken with the ultimate objective of relating the physical properties of the medium to its runability. For this report, runability may be defined as the maximum permissible corrugating speed without fracture of the flutes.

In view of the fact that available knowledge of the corrugating process is largely restricted to machine design and operating variables, this report is of the nature of an exploratory theoretical and experimental investigation of corrugating based on the concept of the stress-strain behavior of the medium. In some specific details the analysis reflects experience with the experimental corrugator at The Institute of Paper Chemistry, although the principles involved should be applicable to any corrugator.

From the mechanics of materials standpoint, corrugating may be viewed as a process wherein an array of machinery imposes sufficiently large stresses and strains on the medium, while forming and subsequently molding it to the shape of a flute under conditions of elevated temperature, so that the medium suffers a permanent set and thereby retains the fluted shape upon leaving the

labyrinth of the corrugating rolls. The molding process may, for convenience, be treated as a two-step process involving (a) formation of the fluted contour, followed by (b) "setting" the flute when it undergoes severe transverse compression at the nip of the corrugating rolls.

The medium fractures if the induced stresses exceed the strength of the medium under the prevailing conditions of heat, moisture, and rate of stressing. It is believed that, in general, rupture occurs during the first steps of molding--that is, about one or two teeth ahead of the center of the labyrinth. At this point the medium, which is under transport, bending, shear and transverse compression strains, has attained nearly the full flute shape but has not yet been subjected to the large transverse compression which takes place at the center of the labyrinth and which "completes" the molding. The intent of this phase of the study, therefore, is to analyze the nature, distribution and, where possible, estimate the magnitude of the stress and strains in the medium during molding and to determine the factors involved in the corrugating process which are important to runability.

The state of stress and strain in the medium during formation of a flute may be considered as the sum of two parts: (a) the tensile stress and strain acquired during transport of the medium from the parent roll to the point where the flute is formed (this stress is sensibly uniform across the caliper of the medium) and (b) the stresses and strains of forming (bending, shear and transverse compression) resulting from severe local deformation of the medium as it attains the fluted shape (bending and shear stresses vary in intensity across the caliper).

In normal operation of the corrugator (used in this study) the transport tension in the medium is maintained at approximately 0.5 pound per inch of web width prior to entry onto the top corrugating roll. The meter which measures this initial tension in everyday operation indicates the average transport tension. It does not show the fluctuating tension due to the impact of the bottom roll on the medium as it enters the labyrinth, which by more elaborate measurements was found to occur at the same frequency as flute formation. Thus, the operating tension (0.5 lb./in.) is a time-average tension; the instantaneous transport tension is periodically greater than this value by the amount of the impact tension. The magnitude of the impact is not well known at this time although this is currently being investigated.

The level of the initial average tension is largely dependent on the force required to unwind the parent roll, overcome friction between the medium and the preheater drum, and overcome friction at the reel brake. A study of the corrugator machine elements associated with web transport indicated that (a) driving the idler rolls, (b) resisting centrifugal effects at idler rolls and other curved surfaces, and (c) support of web weight in free spans between idler rolls are of little consequence in determining the operating level of the initial tension in the corrugator.

The medium travels faster than the peripheral speed of the tooth tips of the corrugating rolls, enabling the draw necessary for the shape of the molded flutes. Each tooth tip in contact with the medium exerts a force of friction on the medium which opposes the draw, resulting in an increment of transport tension in the medium on the leading side of the tooth. The increments

accumulate, with the result that the transport tension approaching the center of labyrinth is elevated beyond the initial average tension ahead of the corrugator rolls. For a coefficient of kinetic friction equal to 0.20, an initial average tension of 0.5 lb./in. would be expected to increase to 1.6 lb./in. for B-flute and to 2.1 lb./in. for A-flute. Furthermore, accumulation of tension is very sensitive to the coefficient of friction. A coefficient of kinetic friction of 0.30, for example, would double the above-mentioned values of tension at the point of complete flute formation. Thus, the coefficient of kinetic friction between the medium and the heated corrugator rolls may be expected to be a significant factor in corrugating. Experiments have shown that it is possible to reduce the coefficient of friction by means of surface additives and therefore reduce the total stress sufficiently to preclude flute fracture at the corrugating speed causing rupture of the untreated medium.

Simultaneously with draw, the medium is formed into the fluted shape of the corrugating rolls whereby very severe deformations are induced in the medium--sufficient to cause large permanent set. An analysis has been made of the bending and shear strains during flute formation, although the analysis probably has more qualitative than quantitative significance because small deflection analysis was employed to describe large deflection behavior. The results of the analysis indicate that formation of the flute does not take place solely by pure bending (this would require a machine-direction stretch of approximately 8%), but involves a combination of bending and shear strain in the medium. The apportionment of strain between bending and shear may be expected to depend on the ratio of the inelastic stiffnesses of the medium with respect to

these two types of deformation. If the medium is relatively stiffer in bending than in shear, flute formation will be accomplished by large shear strain and small bending strain, and vice versa. Comparison of the results of the theoretical analysis and the observed runability of medium on A- and B-flute corrugating rolls suggests that shear strain may be significantly large; therefore, it may be expected that the shear properties of the medium are of importance to medium runability as well as bending properties.

The analysis of bending and shear strains is in qualitative agreement with the observed location of fracture of flutes at the junction of the side wall and the arch when the flute is about one tooth ahead of the center of the labyrinth. Failure due to bending would manifest itself as rupture of the surface fibers, while shear failure would be a delamination at or near the center of the medium. These locations are a result of the distribution of bending and shear strain across the caliper of the medium, namely, maximum bending strain at the surface and maximum shear strain at the centerline of the medium.

No quantitative estimate has been made, at this time, of the magnitude of the instantaneous transverse compression strain at the center of the labyrinth (final step in molding) and its effect on relieving the longitudinal strains in the medium due to the Poisson effect. A comparison of the caliper of medium before corrugating and the caliper at the tip of the flute indicates that the nonrecoverable strain is of the order of 33%.

None of the analyses of significant stresses and strains presented in this report depend on corrugating speed explicitly. And yet runability of a medium is measured in terms of corrugating speed. The relationship between runability and the stress-strain state of the medium involves consideration

of other factors which are dependent on speed. As the corrugating speed is increased, it may be anticipated that the rate of stressing will increase; the temperature of the medium will decrease and the moisture content will increase due to the more rapid passage of the medium through the corrugator. It is reasoned that the effect of changes in these environmental conditions (due to increase in speed) on the induced stresses and strains will be (a) an increase in transport tension because of increased friction and increased impact at the entry of the labyrinth, and (b) a possible change (direction uncertain at this time) in the apportionment of strain between bending and shear. (Consideration of impact at the labyrinth entrance also suggests that fatigue behavior of the medium may be of significance to corrugating.) Furthermore, the increased rate of stressing due to increase in speed may be expected to decrease the allowable strains which the medium can safely withstand, while temperature and moisture changes will probably increase the allowable strains. It is not evident at this time which of the latter two effects will predominate. The combination of changes in the induced strains and the allowable strains may explain, therefore, why a given medium will eventually fracture when the corrugating speed is progressively increased. Work is now in progress to ascertain the sense and magnitude of the several effects noted above.

A complete quantitative determination of stress and strain in the fluted medium was not possible in this exploratory study because of primarily two reasons: (a) lack of adequate information on the instantaneous transport tension (i.e., the increase in average initial tension due to impact of the teeth) and (b) imperfect estimate of forming strains, attributable to use of small deflection theory in the theoretical analysis. Work now in progress is directed

to (a) designing an improved metering device for transport tension and, (b) applying large deflection theory to the analysis of forming strains. However, a complete theoretical determination of corrugating stresses and strains will still be of only qualitative value until such time as the material properties of corrugating medium are better understood. A comparable degree of effort is being directed, therefore, to development of methods for measuring the pertinent material constants, namely, coefficient of kinetic friction and bending and shear stress-strain characteristics under the prevailing conditions of heat, moisture, fatigue, and rate of stressing. Lastly, analysis of the final step of flute molding is in progress. This involves study of the transverse compression induced at the points of driving contact between corrugating rolls and at the centerpoint of the labyrinth and its effect on flow and set of the fluted medium.

The present report is concerned with the state of stress and strain induced in the medium (in contrast to the allowables of the medium) by the corrugating operation up to only the center of the labyrinth. The behavior of the medium from the time it leaves the center of the labyrinth until it emerges from the pressure roll nip is currently being analyzed.

INTRODUCTION

From one standpoint, the corrugating operation may be viewed as merely a means to an end whereby a fluted shape is imparted to a light weight paperboard (medium) for the purpose of providing geometrical separation of two normally heavier weight facings. Viewed in this way, the primary requirement of the corrugating operation is that it produces an end product of satisfactory quality with respect to compression strength, caliper, adhesion, etc.

On the other hand, corrugating is a process and, as such, the characteristics of the progress should be of great significance to the board industry. This is due to the interdependence of (a) economics of the industry, (b) performance of the finished product, (c) properties of the fibrous raw materials (medium and liner), (d) characteristics of the nonfibrous component (adhesive), and (e) the variables of the operation. It is difficult to comprehend, for example, that corrugated board could enjoy its present competitive advantage in the packaging field if corrugating speeds were limited to, say, 50 feet per minute. Indeed, the growth of corrugated containers in this century may be attributed at least as much

to its high volume-low unit cost production as to the performance characteristics of the end product. Philanthropically, the ultimate aim of an industry is directed towards greater utilization through conservation of material. As related to the corrugating industry, this may be interpreted as the production of better boxes through more efficient use of materials. This is highly desirable and is particularly germane to the corrugated box industry which is faced with rising costs and additional competition from the newer packaging materials such as plastics. In some instances, plastics represent a relatively constant cost operation because the increased production has offset the normal increases in cost.

A great deal of development has taken place relative to the corrugating process during the past two decades. Great improvement has been made in the quality of the fibrous components, i.e., medium and liners; attention has also been focused on machine design and operation. For example, a great deal of attention has been given to the study of flute contours which has resulted in improved combined board performance (1, 2, 3, 4, 5, 6, 7). Efficient machine design and plant lay-out have made possible the continuing increases in production capacity. Studies relating to temperature, moisture, adhesive properties, and application, etc. (8) have increased the knowledge of the effect of these variables on the corrugating process as well as production potentials and quality of product. Little attention, however, has been given to the fundamental behavior of the medium during the corrugating process. Wilson (6) has considered the speed differential between the tips of the top corrugating roll and the root of the bottom corrugating roll and has proposed a new flute design which embraces a recessing of the root of the

top roll so that it does not apply a transverse compression to the medium at the tip of the flute. The author states that better quality, higher speeds, better single-faced bond and trouble-free operation have been experienced with rolls of this design.

While much is known about machinery design and operation, relatively little is known about the fundamentals of corrugating in terms of the stresses and strains to which the medium is subjected. That this is a significant area, one may reflect that essentially the array of machinery and its mode of operation are designed for one purpose, namely, to stress the medium to such a degree that it molds, i.e., undergoes a permanent set, and thereby retains a fluted shape while the liners are adhered. Thus, the heart of the corrugating process is basically a matter of the state of stress and strain induced in the medium while in a suitable environment for molding. It may be expected that the limiting factor of corrugating (runability) is directly related to the type and magnitude of the stresses and strains imposed on the medium during corrugating and the ability of the medium to withstand such stresses and strains.

The term runability, as related to corrugating medium, may have several meanings, embracing either or both the process or the end product. Runability has been used by some as an all-inclusive term to denote ability to bond, rigidity of the formed flutes, presence of fractured flutes as well as "high-low" corrugations. It should be readily apparent that runability, as used above, would be related to so many characteristics of the material, operation variables, and technique that the term has no

explicit meaning when used in this sense. In the study reported herein, the term runability is restricted to mean the ability of the medium to withstand the stresses and strains of the corrugating operation without fracture of the flutes. In this case, runability is measured in terms of the maximum corrugating speed at which the medium can be corrugated without fracturing the flutes.

Many corrugator operators are not concerned with runability as defined above because, in their case, the limiting factor is not fracture of the flutes but the presence of excessive "high-low" corrugations. The consequence of "high-low" corrugations (large variation in height of successive flutes) is poor to no adhesion of the low flutes at the double-backer, resulting in a lower quality combined board. Work (9) carried out to date has indicated that "high-low" corrugations appear to be closely related to fracturing of the medium and may also be a direct function of the stress-strain environment encountered in corrugating.

Prompted by the above considerations, The Institute of Paper Chemistry has initiated, on behalf of the Fourdrinier Kraft Board Institute, a fundamental study of the mechanism of corrugating and the behavior of the fibrous and nonfibrous components in the corrugating operation. One of the goals of this study is the determination of the cause of "high-low" corrugations and leaning corrugations as related to the materials and process. From studies of this type may proceed a better understanding of the environments to which a medium is subjected and the relationship between the physical properties of the medium which govern its behavior in terms of runability,

molding, rigidity, and ability to bond readily. Eventually, information of this type may be expected to lead to specification and measurement of those properties desirable in a corrugating medium with implications, perhaps, for selection of the furnish.

The present report is concerned with the analysis of the mechanism of corrugating, that is, the analysis of the stresses and strains imposed on the medium during the formation of the flutes. This report consists of an analysis of the behavior of the medium from the time it leaves the parent rolls until it passes the center of the labyrinth, i.e., the line joining the centers of the top and bottom corrugating rolls, as formed flutes. Additional studies in this area, currently in progress, deal with the stresses and strains imposed on the medium as well as its behavior from the time it leaves the center of the labyrinth until it emerges from the pressure nip as single-faced board. In certain specific details, the current analysis reflects the experience with the experimental corrugator (10) at The Institute of Paper Chemistry. It is believed, however, that the underlying principles are applicable to all corrugators.

The report is divided into three major sections; the first section is concerned with a description of the stress and strain induced in the medium as it passes through the corrugating labyrinth. The second section deals with the estimation of the magnitudes of the stresses and strains imposed on the medium at various locations in the operation. The third section discusses the relationship between runability and the stress-strain state of the medium.

IDENTIFICATION OF CORRUGATING STRESSES IN THE MEDIUM

For the purpose of identifying the nature of the stresses induced in a medium during corrugating, it may be helpful to follow its passage through a machine of current design, as exemplified by the experimental corrugator at The Institute of Paper Chemistry. Figure 1 shows a flow chart for this corrugator. It will be convenient to divide the passage into three stages, namely: (a) from the roll stand A to the point of tangency B on the top corrugator roll; (b) from the point of tangency B to the entry of the labyrinth C (i.e., the region of mesh of the top and bottom corrugating rolls); and (c) within the labyrinth to the point where the flute is fully molded C to D. Point D is the center of the labyrinth, i.e., on the line joining the centers of the top and bottom corrugating rolls. The path which the medium follows as it enters the corrugating nip is shown in Fig. 2 which is a still of one frame of a high-speed movie film showing the medium going through a set of A-flute rolls.

As the medium leaves the parent roll at the roll stand it sustains a tension stress associated with unwinding the roll. This force is necessary to overcome the kinetic friction in the reel bearings and in the brake. Moreover, as the corrugator is brought up to speed, a somewhat increased tension force is required to overcome the inertia of the roll during this acceleration stage. This tension stress may be described as uniform tension in the sense that it is of appreciably constant magnitude across the caliper of the medium.

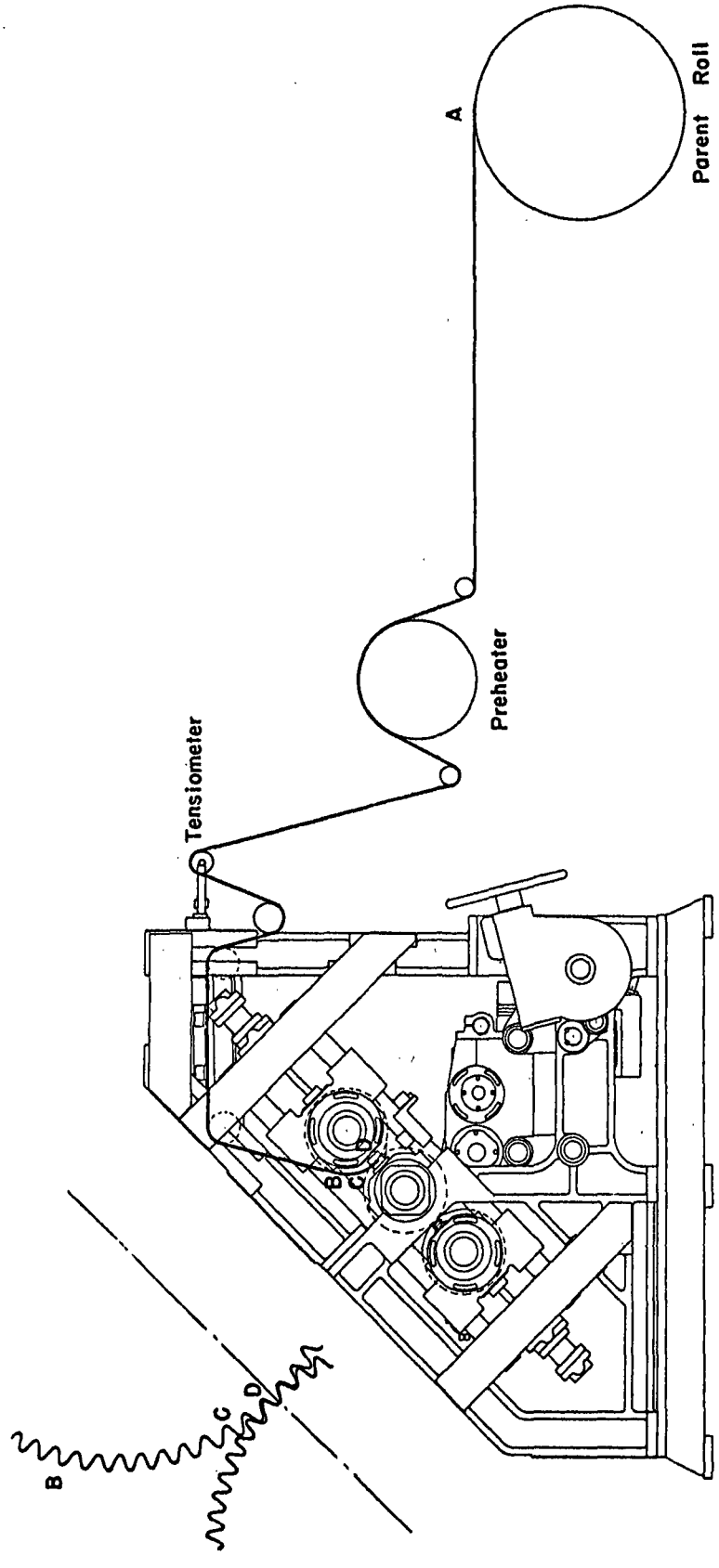

Fig. 1. Path of Medium Through Experimental Corrugator at The Institute of Paper Chemistry

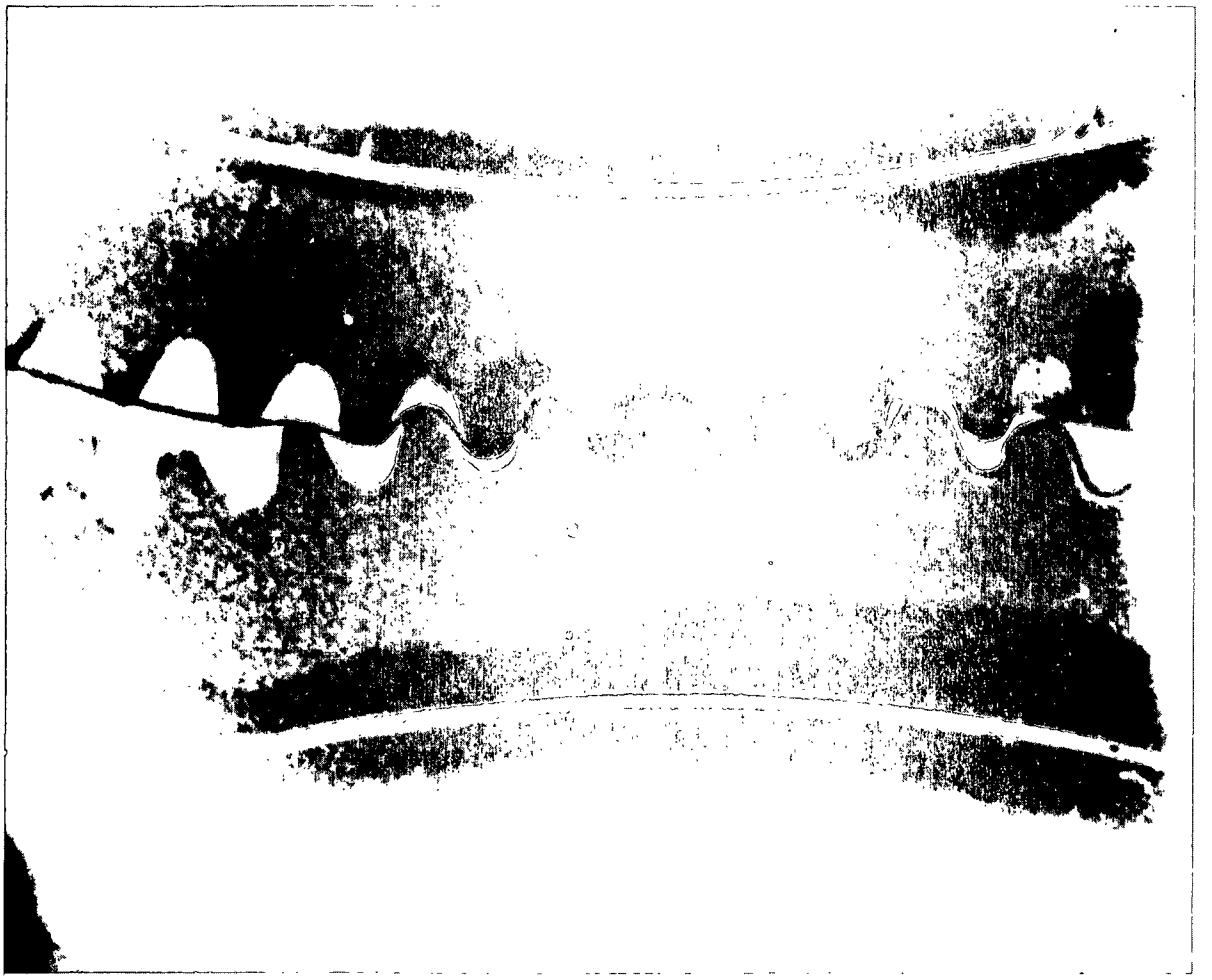

Fig. 2. High-Speed Photograph of Medium in Labyrinth of A-Flute Corrugating Rolls

Over the remainder of its path prior to entry onto the top corrugating roll, the medium passes over a series of idler rolls and a preheater roll. With the exception of the preheater roll, all these rolls are driven by the medium. Each roll has some frictional resistance in its bearings; the medium must provide the force to overcome the bearing kinetic friction. Thus, at each idler roll the medium on the side nearer the corrugator rolls has a somewhat greater tension than on the side nearer the roll stand, as pictured in Fig. 3. That is, there is an increment of uniform tension stress added to the medium at each idler roll due to friction in the roll bearings.

If any of the rolls were fixed rather than free to rotate, a force of kinetic friction would act between the medium and the surface of the roll. Again, an increment of uniform tension stress, associated with overcoming the frictional resistance, would be added to the medium in passing over this type of roll, as pictured in Fig. 4. This latter type of behavior may occur at the preheater. For example, when the preheater is fixed so as not to rotate or rotates at a speed different than the speed of the medium, there is relative motion between the medium and the preheater surface. This causes an increment of tension stress in the medium due to kinetic friction. Even in the case of a motor driven "tracking" preheater, there may be relative motion between the medium and the surface of the preheater because of lack of precise tracking.

As the medium passes over each idler roll, it is bent to conform to the cylindrical surface of the roll. Bending causes stretching of the fibers at the convex (outer) surface of the medium and contraction at the surface

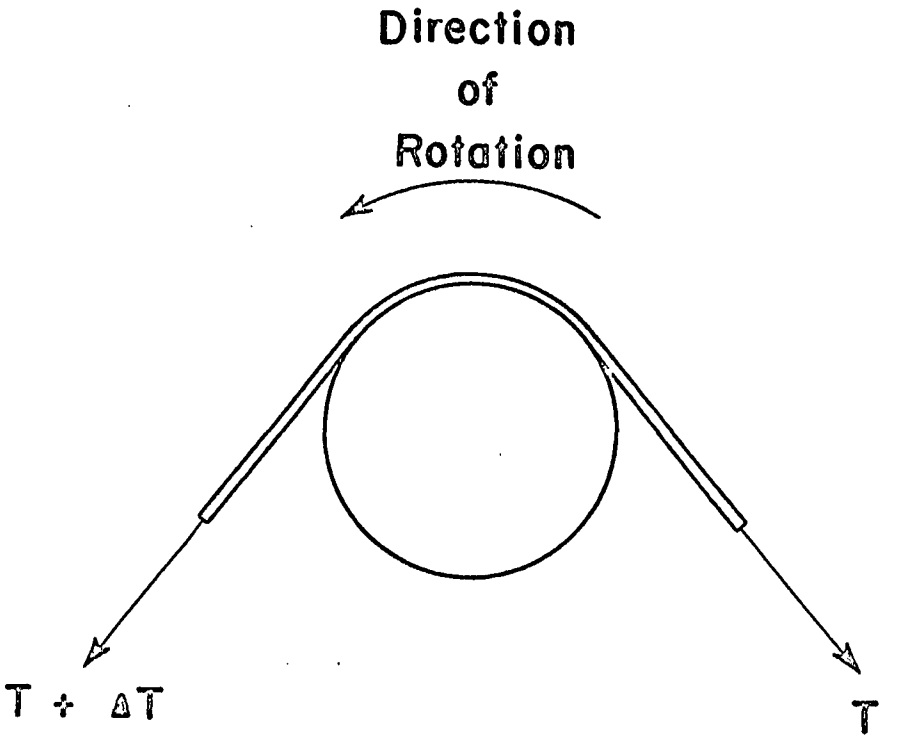

Fig. 3. Increase in Web Tension Due to Friction in Idler Roll Bearings

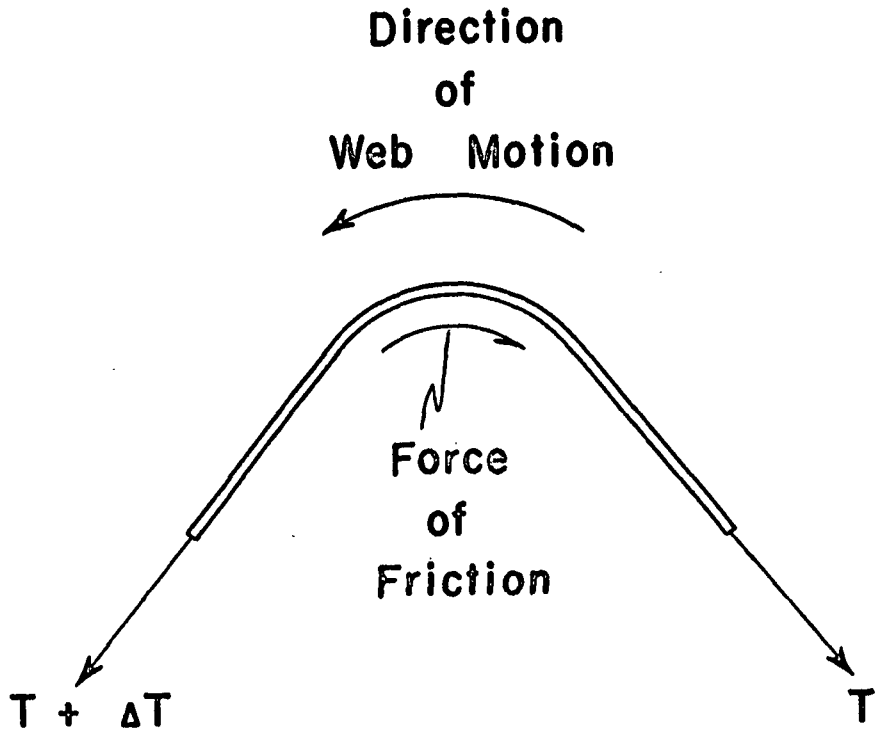

Fig. 4. Increase in Web Tension Due to Friction Between Medium and Surface of a Fixed Roll

adjacent to the roll. Thus, the "half-caliper" on the outside of the bend acquires additional tension stress in addition to that of the uniform tension discussed above, while the inner "half-caliper" sustains compression as pictured in Fig. 5. It may be noted that the stress due to bending progressively diminishes as the neutral axis (i.e., centerline in the case of homogeneous material) of the sheet is approached. Bending is a local stress condition which disappears when the element of medium leaves the idler roll and assumes a straight path to the next idler roll.

Furthermore, as the medium follows a curved path over an idler roll, it tends to be thrown away from the roll because of the centrifugal effect. Each element of medium at this point is constrained to its curved path by the uniform tension stresses in the medium, as illustrated in Fig. 6.

Lastly, the medium must support its own weight in the open span between carrying rolls. A tension force is required to prevent sag of the web over these spans, as diagrammed in Fig. 7.

It should be recognized that the tension stresses identified above are not all additive. For example, the tension force in the medium which serves to overcome bearing friction (and inertia if the medium is accelerating) is sufficient to overcome the centrifugal effect at a carrier roll and to support the weight of the medium in the span between carrying rolls.

If a tension-measuring device (tensiometer) were installed just ahead of the top corrugating roll, it would measure the tension force existing at that location which is sufficient to overcome all of the previous resistances: bearing, brake and/or surface friction, inertia if the web is

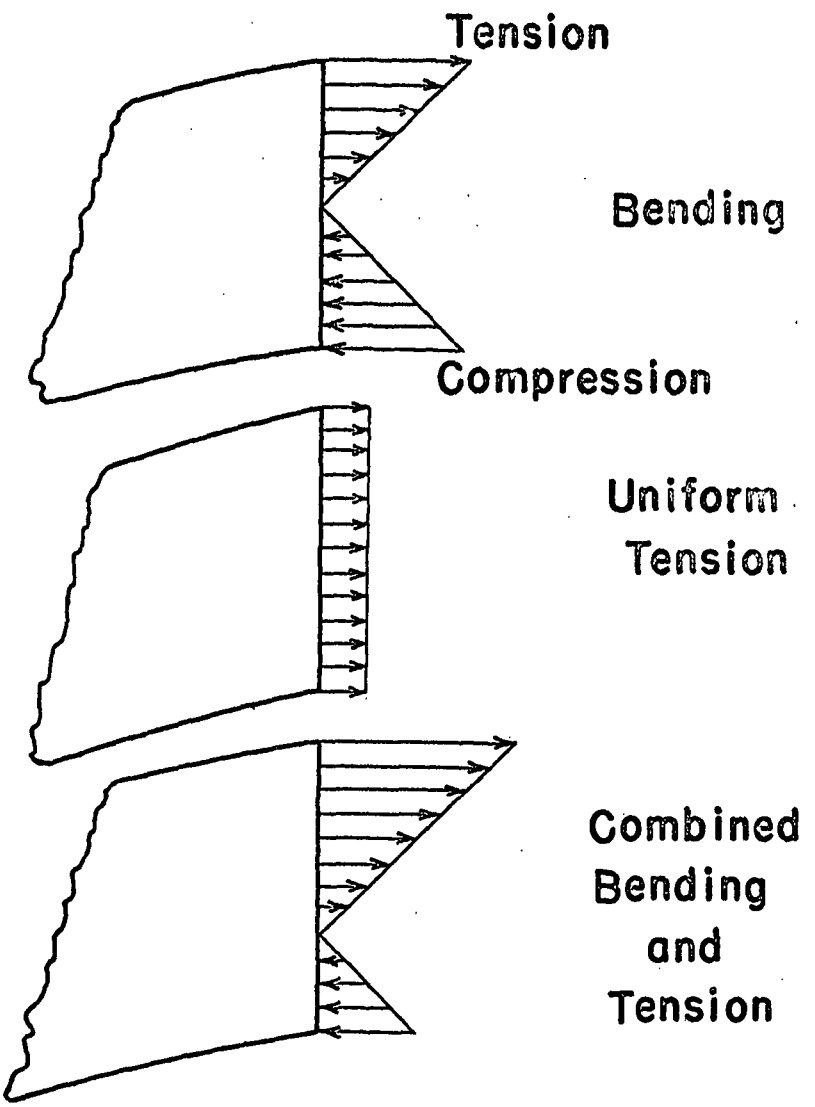

Fig. 5. Combined Bending and Uniform Tension in Medium at Curved Surface of Idler Roll

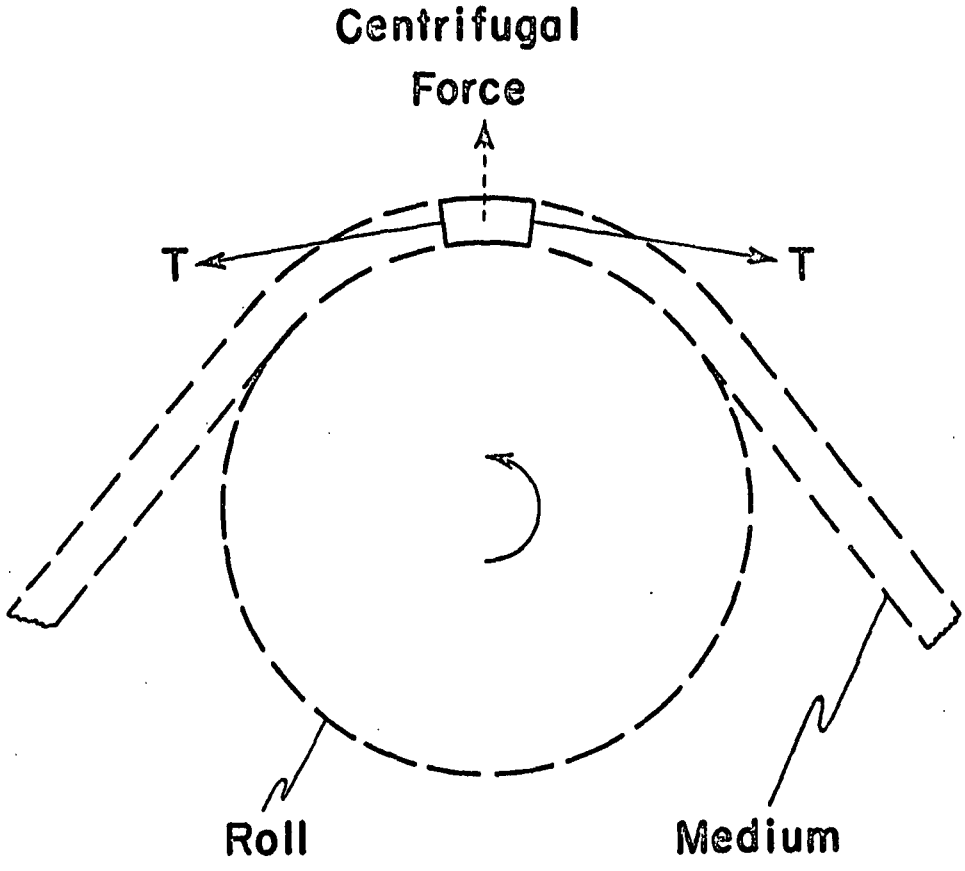

Fig. 6. Web Tension Opposing Centrifugal Force

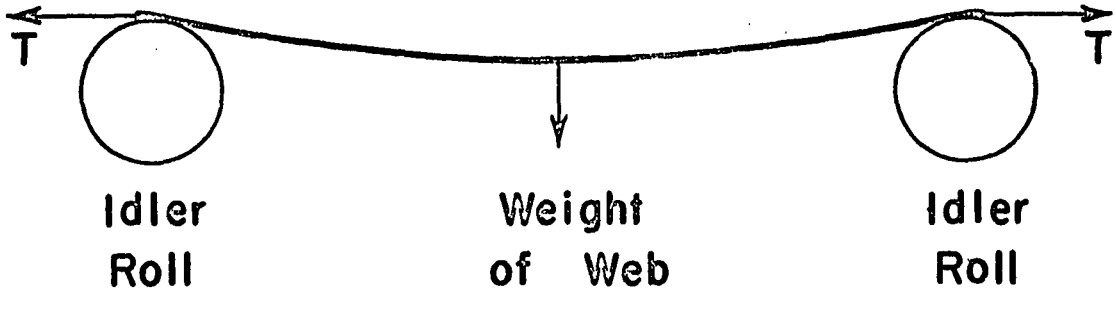

Fig. 7. Web Tension Required to Support Weight of Web

accelerating, centrifugal force, and web weight. Bending, on the other hand, is localized at each carrier roll and is not reflected in the tensiometer measurement. Experimentally, this location of tension measurement has significance; it is the last point prior to formation of the flutes where the uniform tension in the medium may be measured conveniently.

It is common practice in corrugating to adjust the parent roll brake so that the initial web tension force, T_o, in the medium is at some practical but generally unknown level. On the IPC corrugator it has been found desirable to maintain the initial web tension at one-half pound per inch of web width. This operation may be viewed as one of adjusting the total transport resistance (made up of friction, centrifugal force and web weight) so that (a) the medium flows smoothly over the carrying rolls without flutter, wrinkles, or excessive tautness, and (b) a reproducible tension exists in the medium as it enters the stage of flute formation.

The medium flows onto the upper corrugating roll on a line of tangency at point B of Fig. 1 and is transported along the tooth tips (tip of flutes of corrugating roll) to point C where the upper and lower rolls begin their region of mesh. Since the medium is traveling on a curved path from B to C, the tension in the medium must overcome centrifugal force as discussed earlier relative to Fig. 6. Centrifugal tension, however, is not an increment to the total tension beyond point B, Fig. 1; it is equal on both the leading and trailing side of each element of medium and thus is reflected in the tensiometer measurement prior to point B, Fig. 1.

In the region $\overline{BC}$ the medium travels with a greater peripheral speed than the teeth tips. The increased speed of the medium makes possible the take-up (or draw) of the medium, that is, the additional length of medium required to form the fluted contour of corrugated board. Thus, the medium is not merely transported along the upper roll tooth tips, but actually slides past the tips as it is drawn into the contour of the teeth in the labyrinth. There is a frictional drag on the medium, therefore, at each tooth tip between B and C, which increases at each tip resulting in an increased tension on the labyrinth side of each tooth relative to the approach side, as pictured in Fig. 8. At each successive tooth tip the medium acquires an additional increment of tension. In the A-flute experimental corrugator described here, the medium receives 13 or 14 such increments of tension from tooth-tip friction up to the time that it enters the labyrinth.

When the medium reaches point C of Fig. 1 or Fig. 9, it is impacted by the first tooth of the bottom roll in the labyrinth, causing it to deflect laterally and initiates the flute-forming stage of the corrugating process. The short length of medium between two adjacent teeth of the top roll is given an acceleration by the impacting tooth in a direction causing it to deviate from its peripheral path on the top roll. The impacting force will be opposed by a tension stress in the medium on either side of the impacting tooth. This impact tension may be sensed by the tensiometer ahead of the top corrugating roll, provided (a) the sensing element of the tensiometer is sensitive enough to detect and respond to the rapid fluctuations of the impinging teeth, and (b) the impact tension stress is not damped out before it reaches the sensing element.

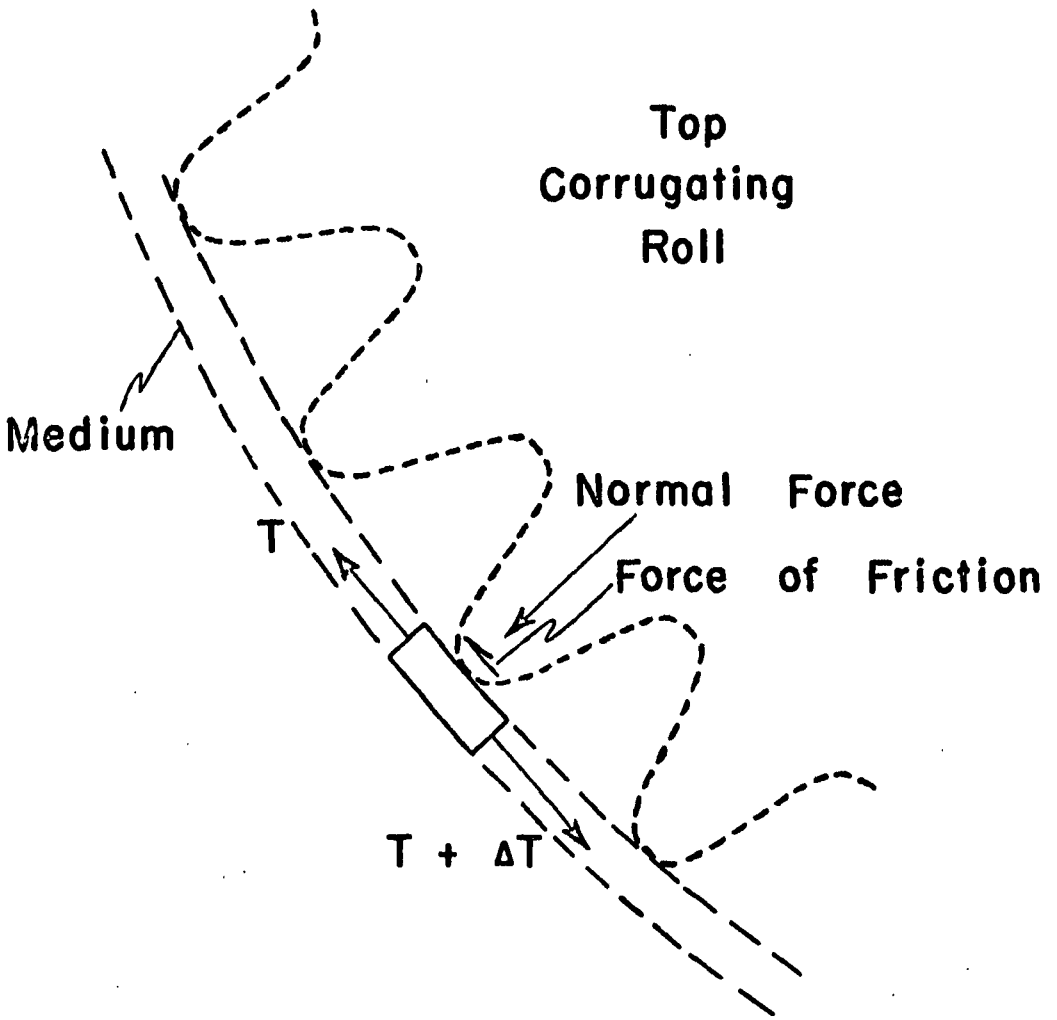

Fig. 8. Increase in Web Tension Due to Slippage Past Tooth on Top Corrugator Roll

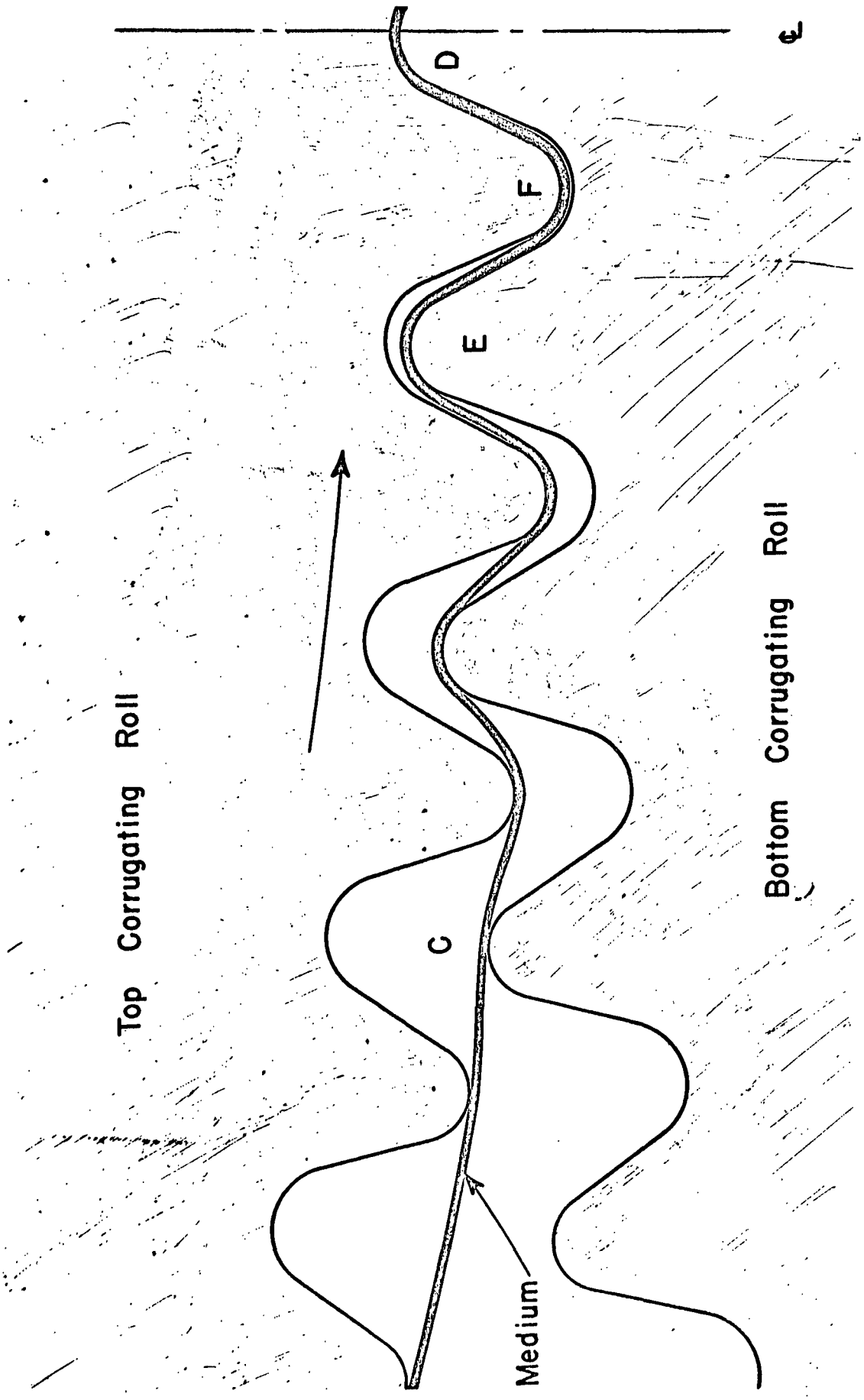

Fig. 9. Labyrinth of A-flute Corrugating Rolls

The medium is literally pulled into the labyrinth $\overline{\overline{CD}}$ and continues to slip past the tooth tips of the labyrinth. From the geometry of the labyrinth, it follows that slippage of the web, which is related to take-up or draw in the labyrinth, necessarily is zero at the center point of the labyrinth, D, Fig. 9. High-speed motion pictures as well as graphical analysis of the labyrinth suggest that slippage may cease at about one tooth tip ahead of the center of the labyrinth. Thus, an increment of tension due to tip friction is added to the medium at each tooth in the labyrinth prior to the tooth of no-slip. As will be shown later, these friction increments become progressively larger with distance into the labyrinth and may accumulate to a substantial total tension force in the medium as the flute-forming operation approaches completion.

When the medium reaches a point such as F of Fig. 9, it may no longer slip past the tooth tip because of the high frictional drag and transverse compression due to the bottom corrugating roll. In this event, the static frictional force at tip F acts on the medium in a direction opposite to those previously considered, that is, the static friction acts in the direction of web travel. This point marks the beginning of the pull exerted on the medium by the corrugating rolls, which provide the motive force of the entire web transport. The following tooth tip D also exerts a pulling force on the web by pinching the medium as well as by static friction. The uniform transport tension in the medium is believed to decrease after point F is passed, since the teeth now provide part of the pulling force, directed along the web. It may be expected that by the time the medium reaches the center of the labyrinth, D, the transport tension is zero or nearly so.

In summary, the medium accumulates transport tension until slippage past the tooth tips ceases. At this point the force of friction is no longer kinetic but static and is acting in the opposite direction because now the tooth tip of the corrugating roll exerts a pulling action on the medium. Beyond this tip, the uniform tension in the medium is believed to decrease and the teeth provide the motive force of the web transport system.

In addition to the transport tensions induced in the medium by friction as it is pulled into the labyrinth, the medium is severely deformed as it assumes the shape of a flute. In molding around the tooth tip, for example, the medium is subjected to bending stresses, whereby the convex (outer) surface of the medium acquires tension stresses and the concave (inner) surface of the medium adjacent to the tooth tip acquires compressive stresses (as discussed earlier for bending around the idler rolls, see Fig. 5.) These bending stresses are additive with respect to the uniform tension stress acquired through transport.

It will be shown later that if flute molding were accomplished solely by bending around the flute tips, the medium would have to withstand stretch in the machine direction at its outer surface in excess of 8 or 9% to be corrugated successfully. This amount of stretch is unreasonably high based on the known machine-direction characteristics of corrugated medium and suggests, therefore, that forming of the flutes is made possible by deformations in the medium in addition to those caused by transport and pure bending. The remaining possible types of deformation are (a) shear and (b) longitudinal expansion in the web along the flute profile due to compression in the transverse direction.

Shear deformation consists of distortion of initially square elements of the medium into diamond-shaped elements, as illustrated in Fig. 10. This type of deformation is produced by mutual sliding of adjacent cross sections along each other and usually accompanies bending. Figure 11 illustrates in a simplified way how bending and shear deformations may complement each other in the flute-forming operation. Figure 11(a) pictures forming due solely to bending which, as already stated, demands unrealistically large elongation of the medium. The illustration applies to a medium which is extremely stiff in shear, that is, a medium incapable of any appreciable shear deformation. Figure 11(b) indicates how forming of the flute would be accomplished solely by shear deformation in a medium which is extremely stiff in bending. It may be expected that forming actually occurs by both bending and shear deformation (as well as uniform stretching due to transport tension), as shown in Fig. 11(c). The apportionment of strain between shear and bending may be expected to be a function of the ratio of stiffnesses of the medium with respect to these two types of strain.

Shear strain tends to delaminate the medium during the forming operation, while bending tends to rupture the medium at the convex surface. The latter type of failure is frequently noted in mediums of unsatisfactory runability.

The presence of shear strain may be seen in photographs taken on a model corrugator at The Institute of Paper Chemistry. This model consists of sectors of two A-flute corrugator rolls made at a scale of 20:1, Fig. 12, and was constructed as a visual aid in studying the behavior of the medium in the labyrinth. In order to maintain geometric similarity with an actual corrugator,

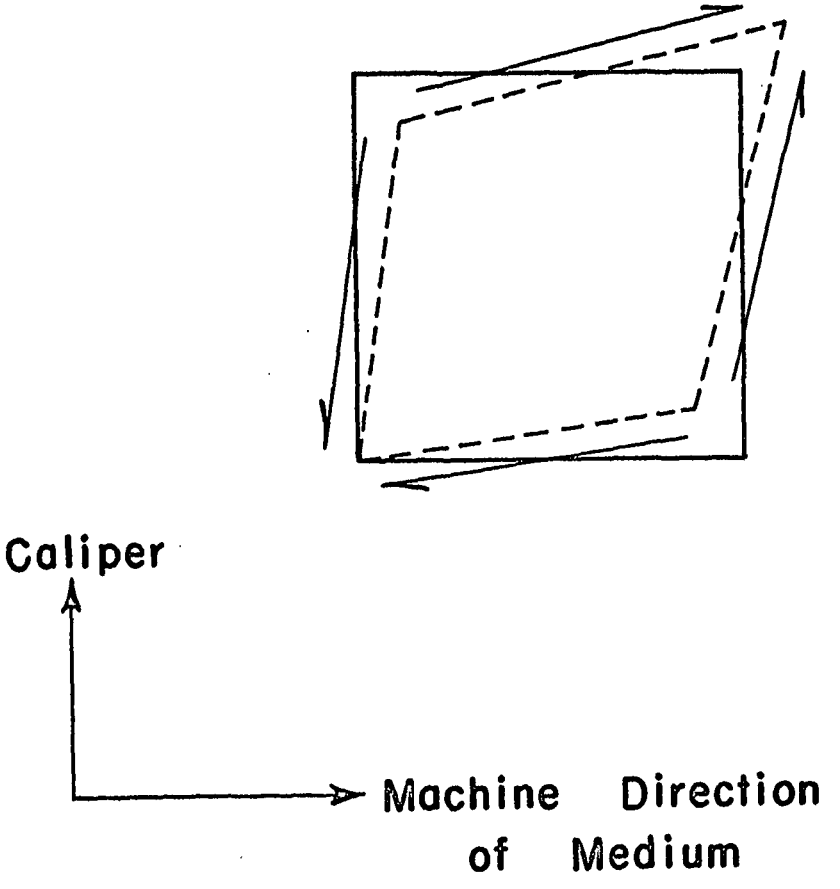

Fig. 10. Nature of Shear Deformation

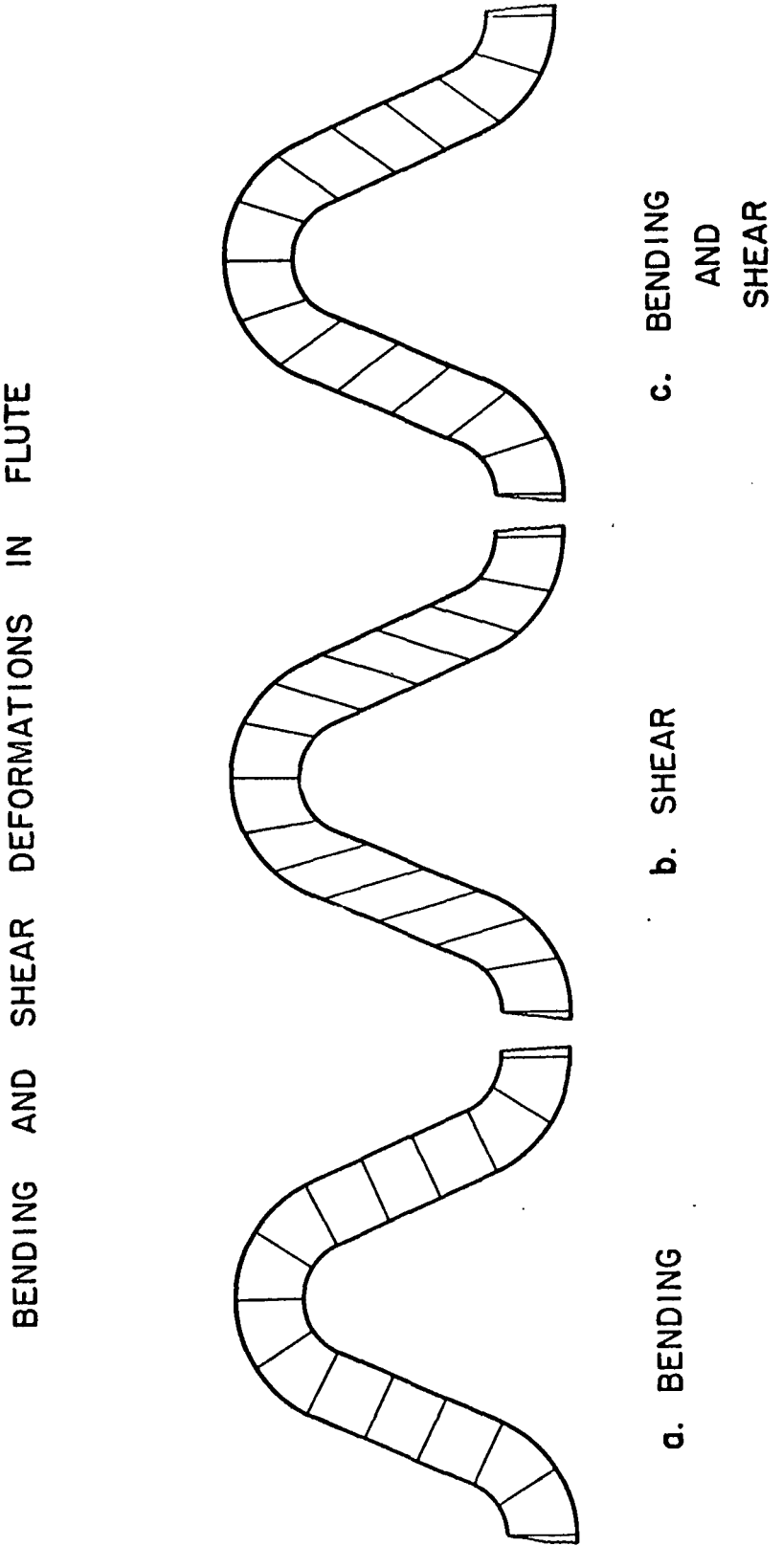

Fig. 11. Bending and Shear Deformation in Flute Molding

Fig. 12. Scale Model of Sectors of Corrugator Rolls (20:1)

a composite medium is used which is formed by assembling a pack of twenty strips of a commercial 26-lb. medium. The strips are not adhered together in any way, so the composite medium has virtually zero shear stiffness.

Figure 13 is a photograph of the model medium at one instant during its passage through the model corrugator. The lines on the medium cross section were initially straight and normal to the medium centerline. The angularity of these lines in Fig. 13 attests to the shear strain which tends to be induced during the flute forming, although the effect is greatly exaggerated in the case of the model.

Returning to actual corrugating, it may be recalled that it is the lower roll which is driving the upper roll, transmitting this driving force through the medium as a tooth approaches the line of centers of the two rolls as well as at the center of the labyrinth. Although the labyrinth configuration illustrated in Fig. 9 was not drawn to show driving contact, the first point of driving contact may be visualized as occurring to the left of tip F. The behavior of the medium at the point of contact may be expected to include two effects: (a) local increase in the shearing strain due to the relative motion of the teeth on either side of the medium at the zone of contact and (b) transverse compression of the medium tending to reduce its caliper within the zone of contact. It may be further anticipated that the medium will elongate somewhat in the machine direction (as a result of the transverse compression) according to Poisson's ratio, a basic material constant. Since the medium is of fixed length from the point of driving contact to a point near D (where the roll clearance becomes less than the medium caliper---normally the clearance is 0.0045 to 0.0060 inch), the aforementioned expansion in the machine direction may bring about some relief in the tensile stress previously induced in the medium.

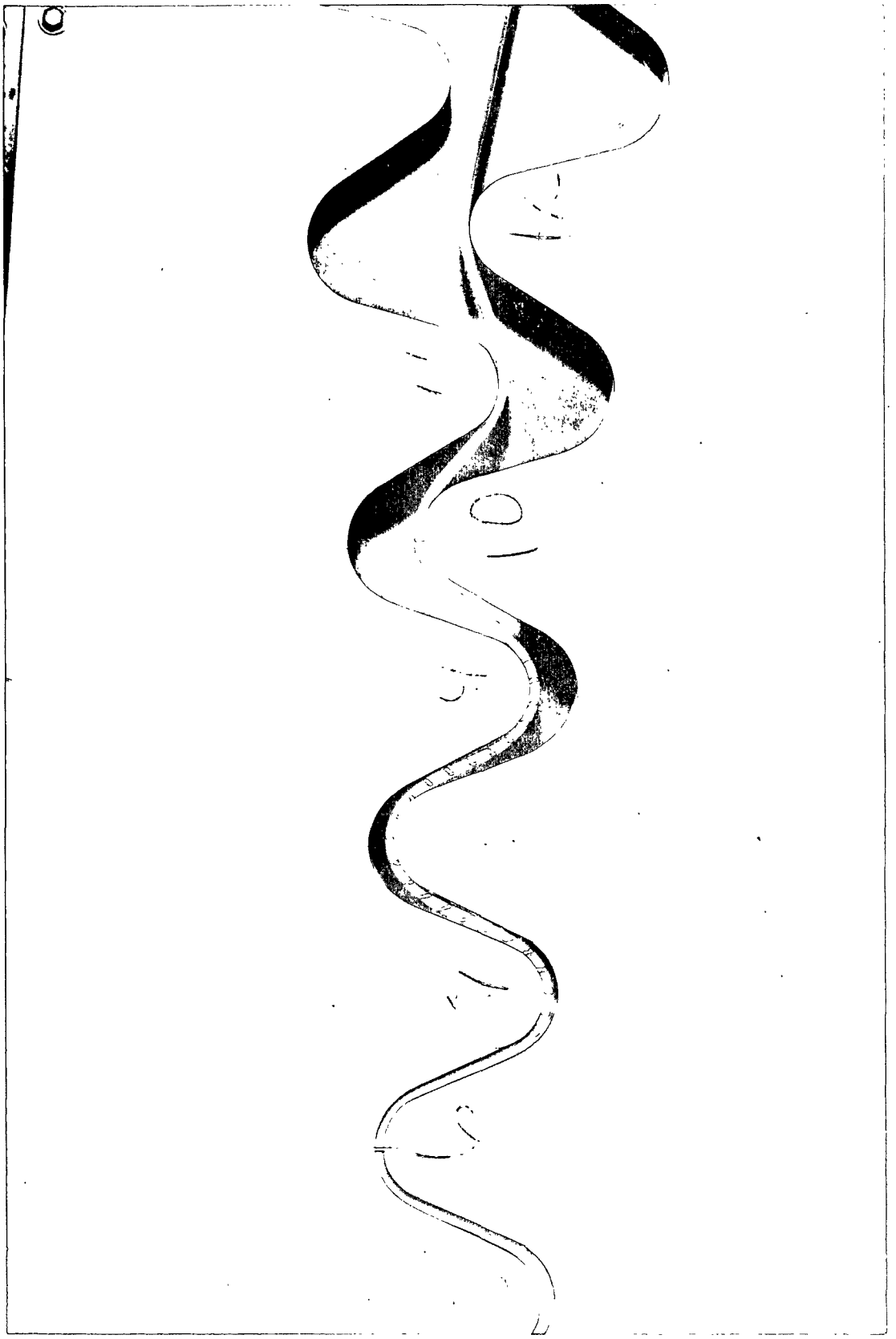

Fig. 13. Photograph of Simulated Medium in Labyrinth of Model Corrugator, Showing Shear Deformation During Flute Molding

The resultant state of stress and strain described above pertains to the medium when it is in the vicinity of one tooth ahead of the center of the labyrinth. At this point (F of Fig. 9) the medium has achieved essentially the shape of the tooth contour and the stresses and strains due to transport, bending, and shear have probably attained their peak intensities. As the flute travels the remaining distance to the center of the labyrinth, D of Fig. 9, the medium probably retains nearly the peak levels of bending and shear strain it incurred at F since the flute shape is basically the same at both locations. There may, however, be some decrease in tension, as discussed above, because unlike earlier locations in the labyrinth the medium is probably not being pulled past the tooth tip representing the first driving contact. Furthermore, there may be some stress relief due to transverse compression (Poisson effect) at the point of driving contact and at the centerpoint of the labyrinth.

By the time the medium reaches point D it has experienced very high bending, shear and transverse compression strains. Moreover, these strains have been acquired while the medium was subjected to high temperature which affects the material properties of the medium and makes it more fluid. At point D, the forces which brought the medium to the state of high stress and strain are rapidly removed. The medium has been strained so highly, however, that because of its viscoelastic behavior it is not capable of returning to its initial plane form, but instead suffers a permanent set which permits it to retain the fluted shape as it proceeds on around the lower corrugating roll to meet the liner.

The principle involved in acquiring the permanent set is probably much the same as is experienced in a conventional tensile test on paper. In this regard, it may be recalled that when a tensile specimen is stressed to a high level such as A of Fig. 14 (but short of rupture) and then unloaded, the load-elongation curve will follow the path $\overline{OABC}$ (11). The branch $\overline{AB}$ of the curve will be traversed during the unloading, and $\overline{BC}$ will be traversed subsequently as a function of time. The distance $\overline{OC}$ is proportional to the permanent set (or nonrecoverable elongation) resulting from the stress cycle $\overline{OABC}$ and represents the amount that the cycled specimen is longer than the virgin specimen.

It may be anticipated that the mechanism leading to permanent set in the tensile test applies in principle to each of the types of strain induced in the medium at the time it passes point D of Fig. 9. That is, an element of medium which was subjected to high tensile strain suffers a permanent set and thereby remains molded after it passes point D. Similarly, an element which was highly strained in shear retains a permanent shear deformation, and analogously for compression. Taken collectively, all elements of the medium remain permanently deformed to a degree approaching the deformation they experienced at points F and D of Fig. 9. Hence, the medium remains in a fluted shape approaching that of the tooth contour.

Based on the foregoing, it would appear convenient to view the flute-molding process as a two-step operation: (a) forming the medium into the shape of the tooth contour, which is essentially completed by the time the medium is about one tooth ahead of the center of the labyrinth, and (b) the setting process associated with the extreme transverse compression

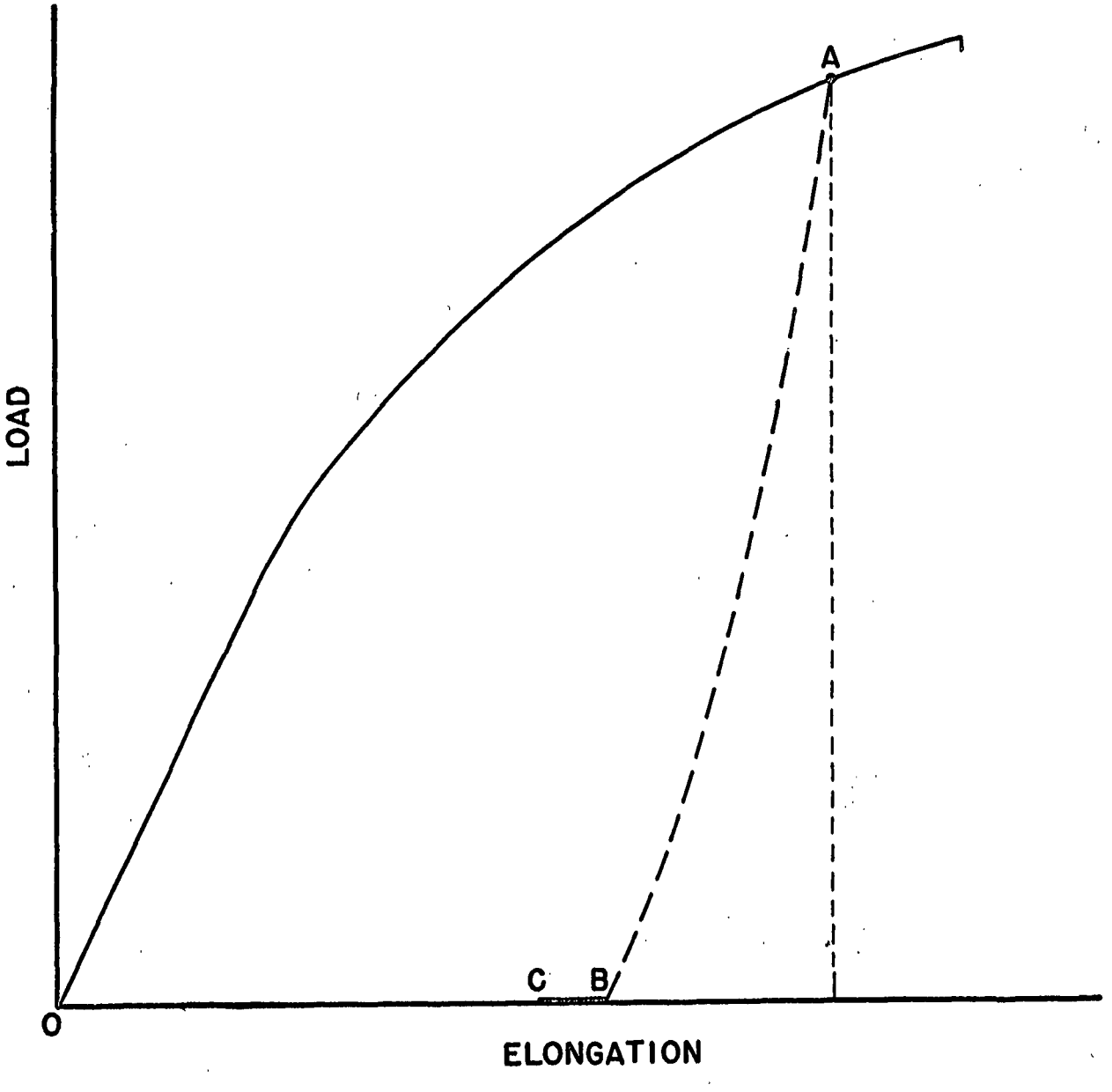

Fig. 14. Typical Tensile Load-Elongation Curve of Paper Under Stress Cycling

imposed at the center of the labyrinth. However, it should be emphasized that these two steps complement one another and there is no clear demarcation of the transition from "forming" to "setting." The latter stage induces a marked flow of the medium because of the elevated temperature of the medium. The flow or permanent set resulting from transverse compression induced at the center of the labyrinth may be noted readily by comparing the caliper of the medium at the tip of the flute with the caliper of the medium before corrugating. Analysis, involving a number of different types of commercial mediums (nominal 26-lb. grade) fabricated into A- and B-flute board, indicates that the caliper of the medium at the tip of the flute is approximately 33 and 37% less, respectively, for A- and B-flute board than the initial caliper of the medium. Thus, the second stage may be looked upon as the operation which completes the molding and is instrumental in locking in the entire complex of strains which have been induced during corrugating.

Separation of flute molding into these two stages has further significance because rupture of medium is believed to occur generally during the forming stage. A limited study employing high-speed motion pictures of the corrugating action within the labyrinth under conditions just severe enough to cause the medium to fracture revealed that rupture occurred one to two teeth away from the center of the labyrinth with the preponderance of rupture occurring one tooth tip away. In these photographs fracture occurred in the vicinity where the arch joins the side wall. Fracture evidently occurred because the combination of stress (or strain) imposed on the medium at these points exceeded the strength (or stretch) of the extreme fiber layer of the medium under the prevailing environmental conditions of heat, moisture, and rate of stressing.

It is significant to note, therefore, that the rupture described above occurred before the final stage of the molding process, that is, before the transverse compression was applied at the center of the labyrinth. Thus, it is believed that rupture is dependent on the first stage of flute molding, during which time the medium is subjected to bending and shear. The remainder of this report, therefore, will be largely concerned with stress and strain in the medium through the first stage of molding, since this stage is apparently directly related to runability in the sense of rupture of the medium.

In the preceding discussion, stresses have been identified which are associated with the steady-state operation of a corrugator. If the corrugator is accelerating, i.e., increasing its operating speed, there will be an increase in the transport tensions in order to overcome the inertia of the several bodies which are driven by the web of medium, that is, the parent roll and the carrier rolls. Moreover, one may anticipate the existence of other transient or perhaps periodic stresses arising in a corrugator. For example, the parent roll of medium may be out-of-round, causing varying tension force in the web as it is unwound. Furthermore, it has been observed that the axis of the top corrugating roll moves periodically relative to the fixed axis of the bottom corrugating roll. This action causes a periodic fluctuation in the clearance between the two corrugating rolls. This variation is probably a manifestation of the varying pitch diameter of corrugating rolls (6) and may be further augmented by variations in the caliper of the medium and variations in the dimension of the fluted contour. If such effects are present, they may cause

variations in web tension which in general are of different periodicity than the stresses induced by forming of the flutes.

It should be recognized that stresses also may arise in the cross-machine direction of the medium, for the following reason. Stresses in the machine- and transverse directions of the medium tend to cause expansion and contraction in the cross-machine direction which may be restrained by frictional forces between the rolls and web, directed parallel to the axes of the rolls. Thus, the medium is probably subjected to a triaxial combination of stresses and strains. In this exploratory study attention is given to only the biaxial combination of stresses and strains associated with the machine and transverse directions of the medium.

ESTIMATION OF MAGNITUDES OF CORRUGATING STRESS AND STRAIN

The preceding section of this report was devoted to identifying the nature of the stresses and strains induced in the medium during corrugating without regard to magnitude. Now an attempt will be made to estimate their magnitudes and thereby deduce the resulting state of stress and strain in the medium when it is molded into a flute. Considerations of this type may be expected to lead to a better understanding of the factors in the corrugating process which are of significance to medium runability and the properties which are to be desired in a medium.

The stress-strain state of the medium during flute formation, i.e., in the labyrinth, may be considered to be the sum of two parts:

I. The uniform transport tension stress or strain induced in the medium during transport from the parent roll to the point in the labyrinth under consideration--uniform in the sense that the tension is essentially constant across the caliper.

II. The nonuniform stress or strain induced in the medium by forming it to the contour of the tooth.

It may be noted that Items I and II do not include all of the sources of stresses in the medium described in the preceding section of this report. For example, local bending occurs in the medium as it passes over an idler roll or other curved surface but disappears when the medium resumes a straight path and thus does not contribute to the stress-strain state in the labyrinth.

TRANSPORT TENSIONS

To systematically investigate web transport tensions it may be helpful to view the web in its entirety. Figure 15 is a diagram of the web as a free body from the parent medium roll to the center of the labyrinth at one instant of time. All of the machine elements have been removed and are replaced by the forces which they are presumed to exert on the web. Straight or curved vectors with half arrowheads denote frictional forces or frictional moments. Dashed vectors are inertia forces (centrifugal, gravitational). The drawing is not to scale; it has certain elements exaggerated (such as the corrugator rolls) to show more clearly the forces acting.

Starting at the parent medium roll, the medium acquires an increment of uniform tension stress each time it passes a frictional moment, i.e., at the roll stand, preheater, and idler rolls. These increments accumulate and just prior to entry onto the top corrugator roll the medium has a total tension, $\underline{T}_o$. As the medium slips around the top corrugator roll it is subjected to a series of frictional forces at each of the tooth tips over which it slides (thirteen or fourteen tooth tips for A-flute rolls on IPC corrugator), of which only four are shown in Fig. 15. An increment of tension force, ΔT, is added to the medium at each of these tooth tips as a result of kinetic friction, as illustrated in Fig. 8. The friction increments continue to accumulate into the labyrinth as long as the medium slides over the tooth tips.

It is of practical significance to consider a tensiometer installed on the corrugator just ahead of the top corrugating roll. A suitable metering device at this location will reveal the total tension, $\underline{T}_o$, in the web prior to

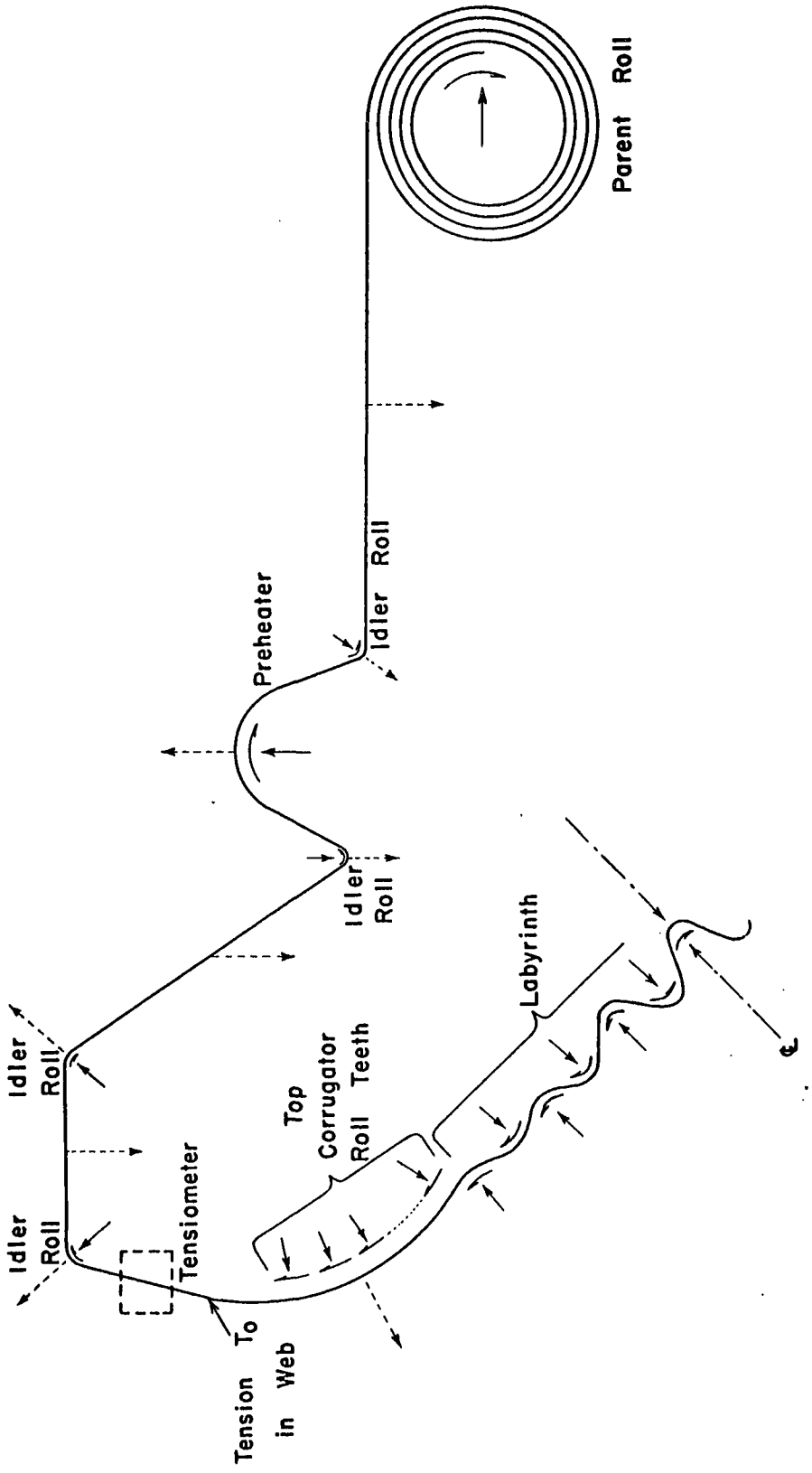

Fig. 15. Diagram of Forces Acting on Medium in Corrugator

entry onto the top corrugator roll. The problem of determining the total (uniform) transport tension at the flute-molding stage then reduces to estimating the additional increments of tension arising on the top corrugating roll and in the labyrinth.

It may be recognized that there is a cyclic variation in the web tension associated with the impact of each tooth of the lower corrugating roll as it enters the labyrinth. This impact diverts the web from its circular path and causes a periodic change in tension in the medium on both sides of the point of application of the impact force. It may be anticipated that this change in web tension will be felt equally at the tensiometer location and within the labyrinth, except perhaps for a difference in damping characteristics of the medium and machine elements on either side of the impacting tooth. Neglecting the question of damping, the periodic variation of web tension within the labyrinth may be expected to be faithfully reflected by the tensiometer provided the meter has sufficient sensitivity to respond to the rapid fluctuations.

In this regard, Fig. 16 shows photographs of the tensiometer signal recorded by an oscilloscope at three speeds with A-flute rolls: 309, 405, and 511 feet per minute on commercial medium. The ordinate is proportional to the force acting in the medium and the abscissa is proportional to time, namely, 0.00579 sec. per division. Table I lists the corrugating speed and corresponding rate of flute formation and the observed frequency of the recorded signal for each photograph. The plus and minus errors on frequency were suggested by several repeat determinations of frequency over various portions of the sweep.

TABLE I

COMPARISON OF RATE OF A-FLUTE FORMATION AND FREQUENCY OF IMPACT FORCE AT TENSIOMETER

Photograph No.	Corrugating Speed, ft./min. [a]	Rate of Flute Formation, flutes/sec. [b]	Frequency of Impact Trace, cycle/sec.	Difference, % [c]
1	309	185	178 ± 4	3.8
2	405	243	232 ± 2	4.5
3	511	307	307 ± 4	0.0

[a] ± 1 foot per minute.

[b] ± 1/2 flute per second.

[c] Based on rate of flute formation.

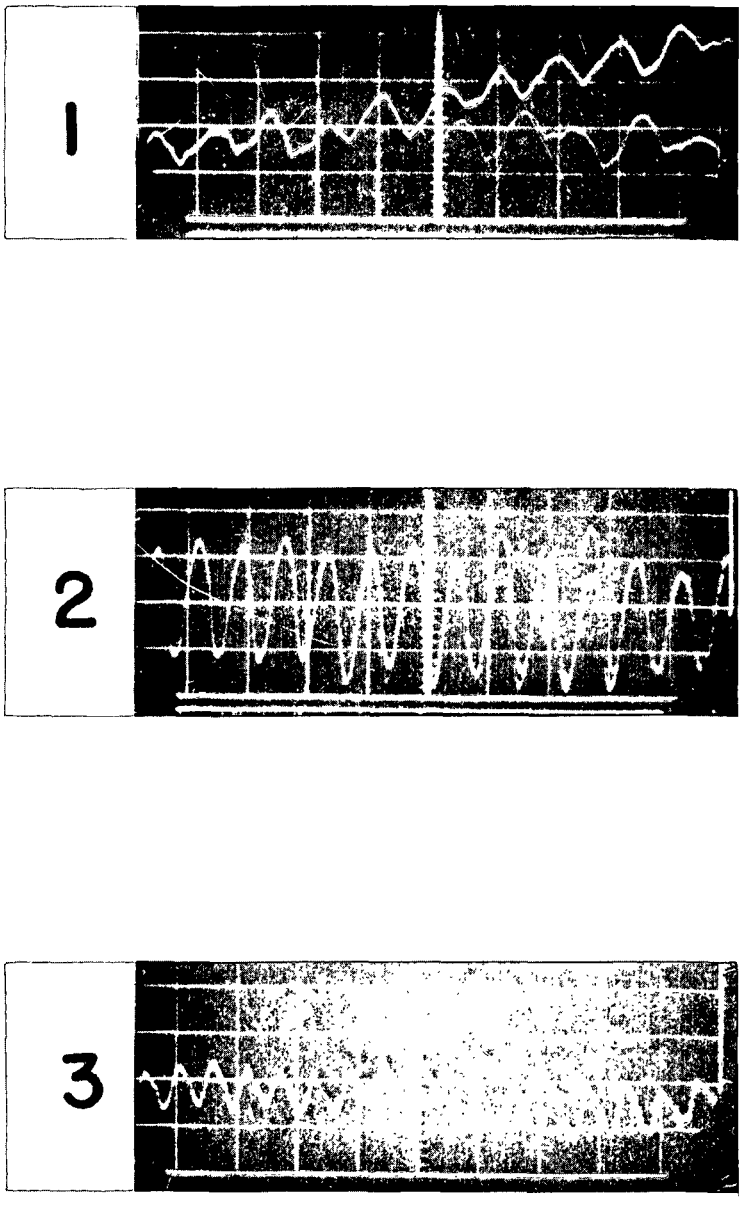

Fig. 16. Photographs of Tensiometer Signal Recorded on an Oscilloscope

It is seen that the frequency of the tensiometer signal is within 5% of the rate of flute formation. Since one tooth of the lower corrugating roll impacts the medium entering the labyrinth once for each flute formed at the nip, it is concluded that the tensiometer indeed senses the impact stresses induced in the medium.

The photographs of Fig. 16 were taken with the zero of the force scale suppressed by an unknown amount. The vertical scale factor is approximately 0.1 lb./in. per scale division in all three photographs, so that the amplitudes of the cyclic variation in the signals may be compared. It may be anticipated that the impact stress would become progressively greater in the absence of damping as the corrugating speed is increased. Thus, the amplitude of Photograph 3 would be expected to be greater than that of Photograph 2, which is not the case. This behavior is currently under investigation.

For everyday usage the tensiometer force is usually indicated on a high inertia meter rather than an oscilloscope. Under these conditions, it is believed that the meter shows the average force on the cantilever beam and suppresses the oscillations shown in Fig. 16. Accordingly, the operator is not aware of the peak-to-peak fluctuations in the initial tension of the medium due to impact at the labyrinth, but is only cognizant of the other "constant" forces associated with web transport. Thus, the initial tension, T_o, which is controlled during the corrugating operation should properly be termed the initial <u>average</u> tension, $\underline{T}_o$. The instantaneous tension may be expected to fluctuate about the average value by

the amount of the impact stress induced by the first impinging tooth of the labyrinth.

It may be noted in Photograph 1 of Fig. 16 that there is evidence that the high-frequency wave is superimposed on a wave of much lower frequency. Investigation of this has indicated that the low-frequency wave is associated with an out-of-round idler roll at the preheater which has since been corrected.

While the meter location shown in Fig. 15 is the preferred location for tension measurements, space limitations demanded that the tensiometer be placed between the preheater and the machine frame in the experimental corrugator at The Institute of Paper Chemistry, as diagrammed in Fig. 1. A consequence of this departure is that three additional friction increments due to three carrier rolls are added to the web after the tension measurement is made. It will be shown that these increments are negligible. Therefore, the IPC tensiometer may be considered as measuring the initial average tension, $\underline{T}_o$, in the web just ahead of the top corrugating roll.

As has been mentioned, the <u>total transport tension</u> (uniform tension) in the medium at the point of flute forming is the sum of (a) tension $\underline{T}_o$ ahead of the tpp corrugating roll and (b) the accumulation of tension increments incurred on the top roll and in the labyrinth as a result of friction. The remainder of this section on Transport Tensions will be devoted to an analysis of the factors which determine $\underline{T}_o$ and estimation of the tension increments on and in the rolls. A later section of the report will discuss the forming stresses which when added to the transport tension complete the determination of the state of stress and strain in the medium at the point of flute formation.

Unless otherwise stated, the following estimates will apply to A-flute corrugation (estimated draw = 1.56) of a 26-lb. medium at a corrugating speed of 500 ft./min. In the inch-pound-second system of dimensions, the basic constants are:

$$w = \text{weight of medium per square inch} = \left(\frac{26 \text{ lb.}}{1000 \text{ ft.}^2}\right)\left(\frac{1 \text{ ft.}^2}{144 \text{ in.}^2}\right) = 0.000181 \text{ lb./in.}^2$$

$$v = \text{speed of web} = \left(\frac{500 \text{ ft.}}{\text{min.}}\right)\left(\frac{1 \text{ min.}}{60 \text{ sec.}}\right)\left(\frac{12 \text{ in.}}{\text{ft.}}\right)(1.56) = 156 \text{ in./sec.}$$

Typical machine-direction tensile properties of a 26-lb. semichemical medium under standard test conditions are:

Tensile strength, lb./in.	35 - 39
Stretch, %	1.3 - 1.5
Proportional limit load, lb./in.	16 - 20
Proportional limit strain, %	0.3 - 0.4
Elastic stiffness (ratio: load/strain), lb./in.	4600 - 5300

Factors Involved in Initial Tension, T_o

The initial tension, T_o, is sufficient to overcome the following forces acting on the moving web.

(1) Centrifugal force

(2) Friction in bearings of reel stand (including brake) and idler rolls, and on preheater drum

(3) Weight of web

It may be of interest to estimate the magnitude of each of these effects so that one may ascertain which are the determining factors in T_o.

Centrifugal Force

As shown in Reference (12), the tension force T in the web required to overcome centrifugal force where the web follows a curved path is

$$T = \frac{w v^2}{g} \qquad (1)$$

where w = weight of web, lb./in.^{2}

v = speed of web, in./sec.

g = acceleratiom due to gravity = 386.4 in./sec.^{2}

It may be noted that the centrifugal tension T is independent of the radius of the curved path. Thus, the centrifugal tension will be the same at each of the carrying rolls, on the parent roll, on the preheater, and on the corrugating roll teeth--depending only on the square of the web speed.

For the corrugating operation under consideration, this component of tension is

$$T = \frac{(0.000181 \text{ lb./in.}^2)(156 \text{ in./sec.})^2}{(386.4 \text{ in./sec.}^2)} = 0.011 \text{ lb./in.}$$

That is, only 0.011 lb. of tension force for each inch of web width is required to overcome centrifugal effects throughout the corrugator when running at 500 f.p.m. Since in practice the initial tension, T_o, is approximately 0.5 lb./in., it is seen that factors other than centrifugal force must determine this level of operating tension.

Since the centrifugal tension depends on the square of the web speed, an increase in the corrugating speed from 500 to 1000 ft./min. would

cause a fourfold increase in centrifugal tension, namely, 0.044 lb./in., which is still only a small portion of the initial tension, T_o.

Friction in Idler Roll Bearings, Reel Bearings and Preheater

Experimental determinations were made of the frictional resistance in the roll bearings of the IPC experimental corrugator, i.e., the rolls which are involved in web transport prior to entry onto the corrugator rolls. These frictional forces are tabulated in Table II and are expressed in terms of the force in pounds per inch of web width required to overcome the frictional resistance. A brief description of the measurements follows:

At the end of a corrugating run a spring scale was affixed to the medium coming off the parent roll of 26.3-inch diameter. With the reel brake disengaged, a measurement was made of the force required to unwind the medium from the roll at a uniform, though low, rate of speed. This force was divided by the width of the roll, giving 0.3 lb./in. as the force required in the web to overcome friction in the reel bearings. (Inasmuch as the force in the web will depend on the radius of the parent roll, this frictional resistance might better be expressed as the moment of friction. This is accomplished by multiplying the above-named force by the roll radius, namely (0.3 lb./in.)(13.15 inch) = (3.9 in.-lb./in.).

The frictional resistance in the bearings of the idler rolls was measured by passing a continuous cloth web belt over the surface of the roll. A weight pan was attached to the belt on each side of the roll. Weights were added to one of the pans until the roll turned with appreciably uniform speed.

TABLE II

FORCE OF FRICTION IN MACHINE ELEMENTS OF THE EXPERIMENTAL CORRUGATOR

Machine Element	Roll Diameter, in.	Web Tension Required to Overcome Friction, lb./in.
Parent roll reel	26.3	0.3 [a]
1st Preheater idler roll	5.5	0.023
2nd Preheater idler roll	5.5	0.010
Tensiometer roll	2.6	0.021
1st Idler roll after tensiometer roll	4.0	0.009
2nd Idler roll after tensiometer roll	4.4	0.023 [b]
3rd Idler roll after tensiometer roll	4.4	0.023
Preheater drums	24.0	1.73 x web tension on low-tension side

[a] Frictional moment = force x roll radius = 3.9 in.-lb./in.

[b] Inaccessible to measurement. Taken equal to 3rd idler roll.

Generally less weight was required to keep the roll turning than to start it in motion, as would be anticipated. The frictions of the five idler rolls were measured by this method, of which two rolls comprise the tensiometer of the I.P.C. corrugator.

As shown in Table II, the force in the web required to drive these carrier rolls is modestly small, ranging from 0.009 to 0.023 lb./in., that is, from about one to two-and-a-half hundredths of a pound per inch of web width. Evidently, the web tension required to unwind the parent roll (0.3 lb./in.) is far more significant than the tension required to drive the idler rolls.

The tabulated values of bearing friction in Table II perhaps should be regarded as estimates of order of magnitude rather than precise determinations of operating constants because actual operating conditions were not fully simulated in the measurements. For example, all the measurements were made at very slow speed, while it is likely that the friction in the bearings may change at the high speeds of normal corrugating. Bearing friction may also depend on axle load and lubricant temperature, neither of which were adequately simulated during the aforementioned measurements.

Lastly, a measurement was made of the frictional force between the tracking preheater drum surface and corrugating medium. It may be recalled that there is frequently a speed differential between the preheater and the moving web so that a force of kinetic friction acts on the medium. For this measurement a loop of corrugating medium with weight pans attached was placed over the preheater drum which was heated to its normal operating

temperature of 360°F. Weight was added to one pan causing slippage of the medium past the drum at nearly constant, though slow, speed.

Inasmuch as the force of friction between drum and web is dependent on the normal forces (which in turn is dependent on the tensions in the web), it is appropriate to consider the ratio of forces on either side of the drum surface rather than their difference. From the measurements described above, it was found that when the tension on one side was 1.73 times the tension on the other side, slippage of the web occurred.

It may be of interest to show that the friction measurements of Table II are reconcilable with actual tension data acquired during corrugating with the I.P.C. experimental corrugator. During a typical run of 26-lb. medium at about 600 feet per minute, the reel brake was adjusted so that the tensiometer read 0.5 lb./in. Tachometer readings showed that the web traveled at 950 f.p.m. and the preheater drum at a peripheral speed of 1025 f.p.m., that is, the preheater speed was maintained higher than the web speed; this is purposely done so that a wide range of mediums can be accommodated without changing the tracking adjustment of the preheater drive. Thereupon, the corrugator was stopped and the force required to unwind the roll <u>against the brake friction</u> was measured immediately with a spring scale. It was found that 0.67 lb./in. was induced in the web in unwinding the roll.

From the data of Table II it is possible to calculate an expected value of the web tension for comparison with the above-named measured value of 0.67 lb./in. at the parent roll. Since 0.02 lb./in. is required to drive the tensiometer roll (see Table II) it is concluded that the web tension was 0.51 lb./in. after this roll and 0.49 lb./in. prior to this roll. Working

backward, the tension prior to the second preheater idler roll was 0.49-0.01 = 0.48 lb./in.--that is, 0.01 lb./in. is required to drive this idler roll, so that the low tension side had 0.48 lb./in. of web tension.

Inasmuch as the preheater drum traveled faster than the web, there was evidently web slippage and the force of kinetic friction acted on the web in the direction of web travel (i.e., opposite in sense to the diagram of Fig. 15). That is, the low tension side of the preheater was on the corrugator side of the preheater. The force on the high tension side (nearer the parent roll), therefore, may be expected to be 1.73 x 0.48 = 0.83 lb./in. Lastly, the first preheater idler roll requires 0.02 lb./in. for driving, so that the web tension prior to this roll and hence at the parent roll may be estimated as 0.83 - 0.02 = 0.81 lb./in. of web width, as compared with a measured value of 0.67 lb./in., a difference of 21%. The magnitude of this difference is perhaps compatible with the precision and degree of simulation of the friction measurements.

Proceeding in the other direction from the tensiometer, the medium passes over three idler rolls in the IPC experimental corrugator before entry onto the top corrugating roll. The total friction of these three rolls is estimated to be 0.009 + 0.023 + 0.023 = 0.055 lb./in. (The second of these rolls was inaccessible to measurement and the friction force is arbitrarily taken as equal to the third and matching roll.) Thus, when the tensiometer reads 0.5 lb./in., it may be estimated that the web tension builds up to approximately 0.5 + 0.05 = 0.55 lb./in. at the point of entry onto the top corrugating roll. This would appear to be an insignificant increase from a practical operating standpoint.

Weight of Web

The uniform tension in the web during transport through the corrugator serves to support the weight of the web in the spans between carrying rolls. According to Reference (13), the relationship between web tension and sag of the web is given approximately by Equation (4), based on the solution of the well-known catenary problem.

$$T = \frac{wL^2}{8d} \qquad (2)$$

where T = tension in web, lb./in.

w = weight of web per unit area, lb./in.^{2}

L = length of span, in.

d = sag of web, in.

Inasmuch as attention is seldom given to specifying the allowable sag of the medium in corrugator operation, it may be well to invert the problem and calculate how much sag may be expected under normal operating tensions. The longest free span in the IPC corrugator is between the parent roll and the preheater. For a typical parent roll diameter this span is 96 inches. Evaluating Equation (4) with a tension of 0.67 lb./in. (see discussion of preceding section) it is found that for a 26-lb. medium, the sag d may be expected to be

$$d = \frac{wL^2}{8T} \qquad \frac{(0.000181 \text{ lb./in.}^2)\ (96 \text{ in.})^2}{8\ (0.67 \text{ lb./in.})} = 0.31 \text{ inch.}$$

A measurement of sag in this span under these operating conditions yielded $d = 0.5$ inch, approximately. This was a difficult measurement to make because (a) the web frequently was concave upward or downward across the width, making a line-of-sight measurement difficult, and (b) out-of-roundness of the parent

roll make it difficult to establish a constant reference line. Nonetheless, the estimated and calculated values are of the same order of magnitude and lend credence to the estimate.

It is presumed that excessive sag in the web may lead to undesirable aerodynamic effects in medium transport such as flutter. Other than this possibility, it appears that web weight is not an important factor in determining operating tensions in a corrugator.

In summary, based on experience with the experimental corrugator at The Institute of Paper Chemistry, it appears that the level of initial average tension in the medium prior to entry onto the top corrugating roll is largely dependent on the force required to unwind the parent roll and the force of friction between the medium and preheater drum. In a typical corrugating run, the force to unwind the parent roll was doubled by means of a reel brake, and the motor-driven preheater was employed to pull the medium off the reel. Between the preheater and the top corrugating roll, the tension in the medium was sensibly constant at its nominal prescribed value of 0.5 lb./in. Driving the idler rolls, resisting centrifugal effects, and support of web weight in free spans between rolls appeared to be inconsequential in so far as determining the level of initial tension is concerned.

Accumulation of Transport Tension Due to Friction of Corrugator Rolls

The medium enters onto the top corrugating roll with an initial average tension T_o (usually about 0.5 per inch of web width). Because of the

draw which takes place in the labyrinth, the medium slips past the tooth tips of the top corrugating roll and continues to slip past the tooth tips of both rolls within the labyrinth until a point about one tooth from the nip has been reached. Each tooth tip exerts a force of friction on the medium in a direction opposite to the direction of web travel. In overcoming this friction force, a greater web tension must exist on the labyrinth side of the tooth than on the tensiometer side, as pictured in Figs. 8 and 17.

According to Reference (14), the high-side tension, T_2, is related to the low-side tension, T_1, by

$$T_2 = T_1 \, e^{\mu\beta_1} \qquad (3)$$

where T_2 = higher tension, lb./in.

T_1 = lower tension, lb./in.

e = base of Naperian logarithms = 2.718+

μ = kinetic coefficient of friction between corrugating medium and tooth tip, dimensionless

β_1 = angle subtended at center of tooth tip by curve of contact between medium and tip, radian.

See Fig. 17. Thus, at the first tooth tip on the upper corrugating roll

$$T_1 = T_o \, e^{\mu\beta_o}$$

where T_o is the measurable tension given by the tensiometer.

At the second tooth tip

$$T_2 = T_1 \, e^{\mu\beta_1} = (T_o \, e^{\mu\beta_o}) \, e^{\mu\beta_1} = T_o \, e^{\mu(\beta_o + \beta_1)}$$

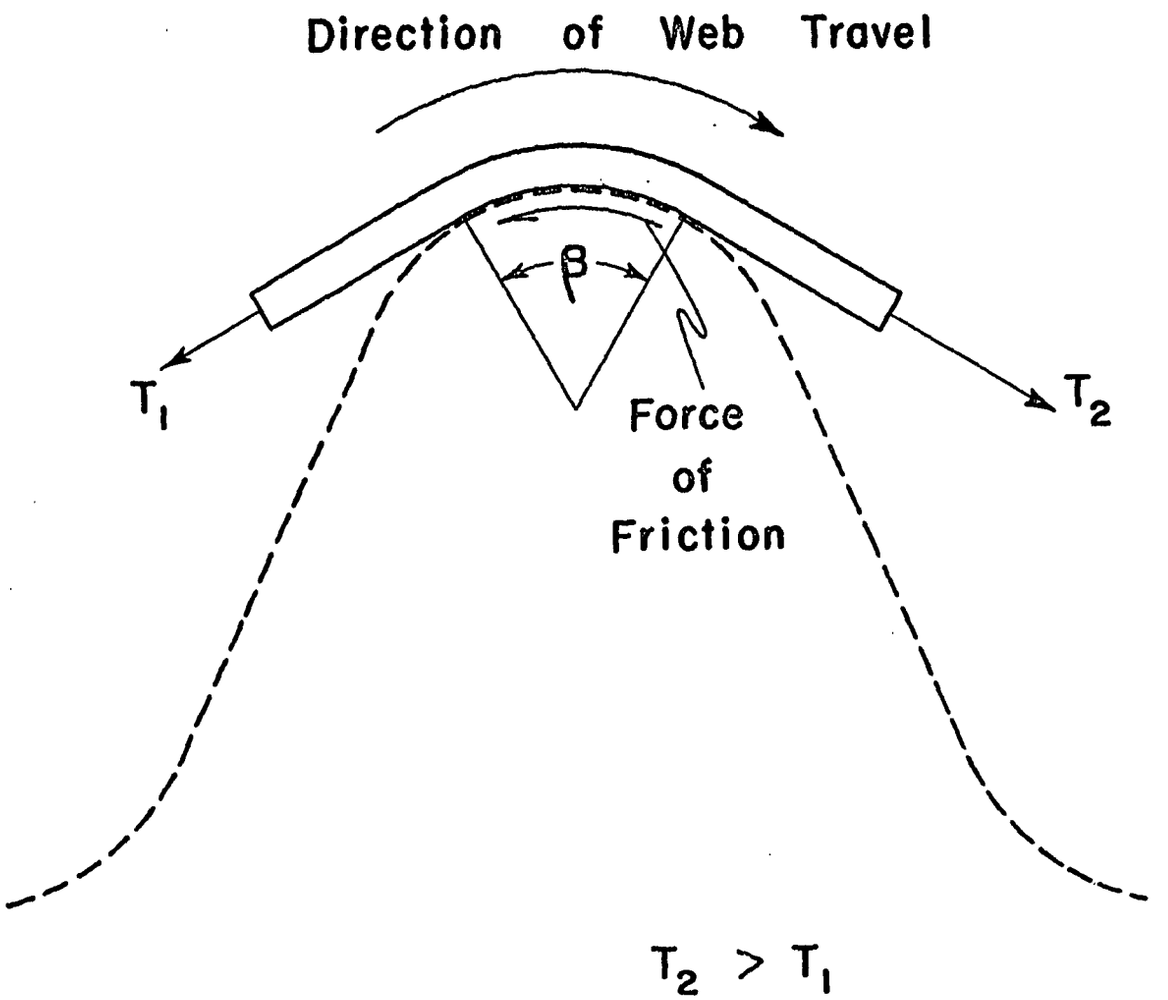

Fig. 17. Parameters Employed in Friction Analysis at Tooth Tip

and at the third tip

$$T_3 = T_o \, e^{\mu(\beta_o + \beta_1 + \beta_2)}$$

After the nth tip has been passed, the tension in the web is

$$T_n = T_o \, e^{\mu(\beta_o + \beta_1 + \cdots + \beta_{n-1})} \qquad (4)$$

Thus, the average tension existing in the medium after it has slipped past a given number of teeth can be calculated from a knowledge of the initial tension, T_o, kinetic coefficient of friction, μ, and the angles of contact at each of the tooth tips. It is possible, therefore, to estimate the total transport tension existing in the medium at any point on the top corrugating roll or in the labyrinth. Of particular interest, of course, is the maximum tension, T_m, in the final stages of flute formation where fracture of the medium may occur.

Determinations of total tension were made for the A- and B-flute contours employed with the IPC experimental corrugator. The numerical data obtained in these analyses are presented in Appendix A. In brief, the method was as follows: For each of the flute contours a 20:1 graphical construction of the labyrinth was made, based on dimensions given on the cutter blueprints used in machining the rolls. A nip clearance of 0.006 inch was used. A series of labyrinth drawings were made for each flute contour, corresponding to various angular rotations of the rolls during passage of one flute past the line joining the roll centers, i.e., the centerpoint of the labyrinth. Specifically, drawings were made for the following locations of a tooth tip of the bottom roll:

1. At the centerpoint
2. 1/8 Flute-width ahead of the centerpoint
3. 1/4 Flute-width ahead of the centerpoint
4. 3/8 Flute-width ahead of the centerpoint
5. 1/2 Flute-width ahead of the centerpoint
6. 3/4 Flute-width ahead of the centerpoint.

For each of these labyrinth configurations the path of the medium was sketched in, thereby enabling estimation of the β angles. (Outside the labyrinth, the β angles are constant and equal to the angle subtended at the roll center by one flute width.) Determination of the medium path was facilitated by a double straight-edge of width scaled up from 0.010 inch. The path of the medium between successive tooth tips was obtained by laying the straight edge tangent to both teeth.

After the β angles were read, the total tension was calculated from Equation (4) for several assumed values of kinetic coefficient of friction, μ. Determination of the farthermost tooth into the labyrinth where slippage occurs was accomplished by inspection of each labyrinth drawing. If, for example, the medium was not fully seated in the root of the roll profile, it was presumed that slippage must occur on the preceding tooth tip, thereby permitting the flute in question to attain its full height. If, on the other hand, the medium was fully seated in the root (and this occurs ahead of the centerpoint because at the centerpoint the medium caliper is compressed to less than its initial value) then the previous tooth tip must be a tip of no-slip. It was found that the tooth of no-slip was approximately one tooth ahead of the centerpoint of the labyrinth.

The graphical constructions of the labyrinth described above, however, fail to simulate one aspect of corrugator roll operation, namely, the driving action of the lower roll against the upper roll (through the medium caliper) at a point to the left of F in Fig. 9. This driving action introduces a differential angle of rotation between the two rolls which was not accounted for in the drawings. It is believed, however, that under driving action the total angle of contact at a given tooth tip will not differ appreciably from the graphical determination.

Figure 18 shows graphically the results of the friction determination described above for A- and B-flute. Each curve shows the ratio of the maximum transport tension, T_m, to the initial tension, T_o, prior to the corrugating roll as a function of the kinetic coefficient of friction of medium against metal. Tension, T_m, is distributed uniformly across the caliper of the medium. It is seen that a sizable growth in tension is attributable to friction on the corrugating rolls. If the kinetic coefficient of friction were 0.2, for example, $T_m/T_o = 4.1$ for A-flute; that is, the transport tension builds up to 4.1 times its initial value. For an initial tension of 0.5 lb./in., the final uniform tension in the web may be expected to reach $T_m = (4.1)(0.5) = 2.1$ lb./in. If the initial tension T_o were maintained at 1.0 lb./in., the final transport tension in this case may be expected to be 4.1 lb./in.

Figure 18 reveals that the final tension, T_m, increases rapidly with increase in the coefficient of friction between the medium and the heated rolls--exponentially, as seen from Equation (4). For the case considered above, a coefficient of 0.3 yields a ratio $T_m/T_o = 8.5$, giving a

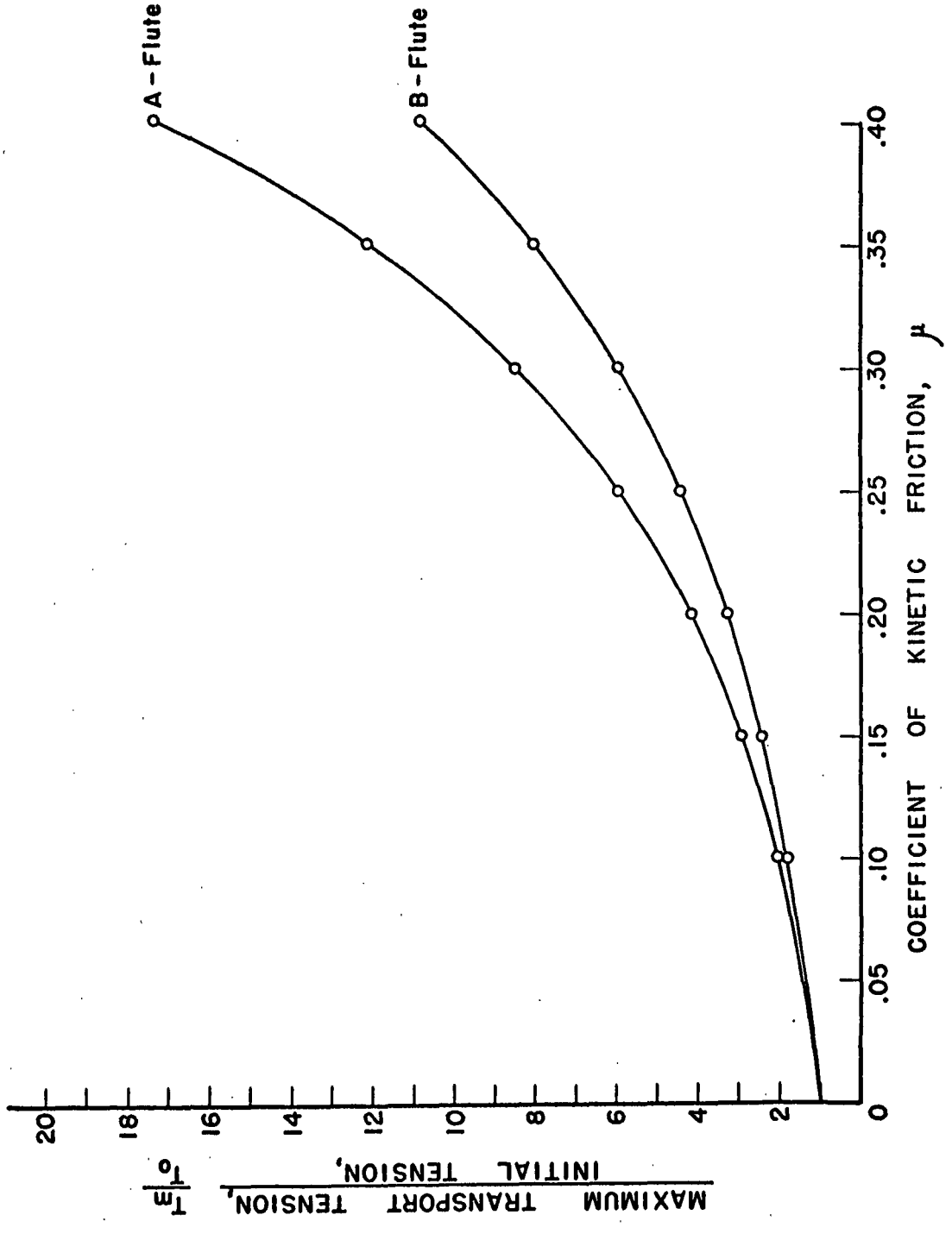

Fig. 18. Maximum Transport Tension in Labyrinth as a Function of Coefficient of Kinetic Friction for A- and B-Flute Contours

total tension of 4.25 lb./in. when the initial tension is 0.5 lb./in. and a total tension of 8.5 lb./in. for an initial tension of 1.0 lb./in. Thus, a 50% increase in coefficient leads to about a 100% increase in transport tension inside the labyrinth. These observations suggest that the kinetic coefficient of friction of the medium may be expected to be a significant factor in the intensity of stress induced in the medium during transport through the corrugator.

Comparison of A- and B-flute in Fig. 18 shows that the A-flute sustains the greater total tension inside the labyrinth. For 0.5 lb./in. initial tension and $\mu = 0.2$, 2.1 lb./in. tension would be induced in the A-flute and 1.6 lb./in. in the B-flute--a difference of 30% based on the B-flute tension. The per cent difference would increase at higher coefficients of friction. The sense of the differences noted is attributable to the greater tip radius of the A-flute tooth (0.0582 vs. 0.0490 in.) and hence a greater angle of contact β, and therefore a greater total frictional force at the tip.

The values of T_m/T_o plotted in Fig. 18 correspond to the one angular orientation of the corrugating rolls out of six which gave the maximum value of the ratio. One may ask: What is the state of total tension at intermediate orientations? It is indeed conceivable that higher ratios of T_m/T_o may be obtained at positions intermediate to those studied. Unfortunately, a cross-plot of T_m/T_o vs. position does not afford a satisfactory interpolation of the ratio at all intermediate positions because of discontinuities in the curve. A rough interpolation, however, suggested that at $\mu = 0.20$ the T_m/T_o ratio may be as great as 4.6 for A-flute rather than 4.1. It should be recognized, therefore, that the final transport tensions may be somewhat greater than predicted by the curves of Fig. 18.

Finally, it may be noted that the final average transport tension is a fairly modest percentage of the tensile strength of a typical medium. Limiting attention to friction coefficients no greater than 0.30, it is seen in Fig. 18 that the maximum value of T_m/T_o is 8.5. If the initial tension T_o were maintained at 1.0 lb./in., the maximum transport tension in the labyrinth would be 8.5 lb./in. Typical 26-lb. semichemical mediums have a tensile strength in the range of 35 to 39 lb./in. in the machine direction under standard test conditions. The extreme transport tension considered here is of the order of 20 to 25% of the tensile strength of the medium. Thus, the data presented on transport tensions are in accord with the rather obvious conclusion that a medium does not rupture due to solely transport tension under normal corrugator operation.

Even though the transport tension may not be extremely large, it contributes to the total stress in the medium. A critical state of stress and strain may be reached when the bending stresses, resulting from bending the medium to the contour of the fluted roll, are added to the transport tension. In this sense, an increase or decrease in the transport tension may determine whether or not the medium fractures during formation of the flutes. For example, the observation that A-flute is frequently more susceptible to rupturing than B-flute under same environmental conditions in commercial corrugating may be a consequence of the greater friction in the A-flute labyrinth, as noted above.

It has been shown experimentally with the IPC experimental corrugator that it is possible to increase the runability of a medium by decreasing the kinetic coefficient of friction of the medium. In several instances,

application of a silicone spray to one side of the web permitted increases in corrugating speed ranging from 100 to 300 ft./min. at the 500 ft./min. level (15). Similar results have been experienced in commercial operations through the use of additives such as graphite and oil mist (16). In view of the preceding discussion of friction effects, these experimental results may be explained as follows: a decrease in transport tension was achieved by means of the silicone or other friction-reducing agents and therefore the total stress was reduced sufficiently to preclude flute fracture under the environmental conditions which caused rupture of the untreated medium.

Laboratory evaluation (15) of the coefficient of kinetic friction between typical corrugating mediums and a chrome-plated surface heated to 390°F., gave an average coefficient of 0.23. As an independent check Equation (3) was utilized in computing the coefficient of friction from the friction measurement taken on the preheater drum as previously described. In this case, the ratio of forces, T_2/T_1, causing uniform slippage was determined experimentally to be 1.73 for the particular semichemical medium used in this study. The angle of contact is approximately 180° (i.e., π radians). Equation (3) may be solved, therefore, for μ, yielding an estimate of the coefficient of kinetic friction of corrugating medium on the heated (360°F.) drum. That is,

$$\mu = \frac{1}{\pi} \log_e \left(\frac{T_2}{T_1}\right) = \frac{\log_e 1.73}{\pi} = 0.174$$

For want of more extensive information on the coefficient of kinetic friction of medium passing over a heated metal surface, a value of $\mu = 0.20$ will be used in the remainder of this report.

Taking $\mu = 0.20$ and initial tension $T_o = 0.5$ lb./in., the maximum transport tensions at the stage of flute forming are:

Flute	Maximum Average Transport Tension, T_m, lb./in. [a]	Maximum Average Transport Strain, % [b]
A	2.1	0.044
B	1.6	0.034

[a] Corresponding to initial tension of 0.5 lb./in.; "average" in the sense that impact tension is not included.

[b] Based on elastic stiffness, $E_t = 4750$ lb./in.

It is seen that these transport tensions and strains are but a small fraction of the proportional limit load and strain of a typical 26-lb. medium under standard test conditions, namely, 16 to 20 lb./in. and 0.3 to 0.4%. It must be emphasized, however, that the magnitudes of these material properties probably change under the environmental conditions of corrugating.

BENDING AND SHEAR DURING FORMING

The preceding discussion of transport tensions was concerned with the uniform tensions induced in the medium during its travel to approximately the center of the labyrinth, as distinguished from the bending and shear stresses incurred during the severe deformation of the medium into the fluted shape. It was concluded that the initial average tension, T_o, (usually 0.5 lb./in. of web width) existing in the web before entry into the corrugating

labyrinth was largely attributable to unwinding the parent roll of medium and passage over the preheater. Draw of the medium into the labyrinth elevated the initial uniform tension to a higher value, T_m, because of kinetic friction at the tooth tips. It was estimated that an initial average tension of 0.5 lb./in. would be increased to 1.6 - 2.1 lb./in. by the time the medium reaches a point one tooth from the centerpoint (for a friction coefficient of 0.20). The instantaneous tension may be expected to be larger than these values by the amount of the tension induced by the impacting tooth of the lower roll as it enters the labyrinth.

Simultaneously with the above-mentioned draw, the medium is progressively bent into the shape of the flute. Stresses are induced during the bending which must be added to the transport stresses to obtain a complete description of the state of stress and strain in the medium. As mentioned previously, these stresses and strains may be expected to include bending, shear, and compression. Rupture of the medium occurs if the stress and strain imposed on the medium exceed its strength under the prevailing environmental conditions of temperature, moisture content and rate of stressing.

The medium is reasonably plane when it enters the labyrinth (radius of curvature of approximately 6 inches) while at the completion of flute forming it is severely deformed to the contour of the roll tooth. If flute formation were to be accomplished solely by bending, the medium would behave as illustrated in Fig. 19, which shows one half of a flute, beginning at the mid-point of one side wall and ending at the mid-point of the successive side wall. The flute pictured here is prior to the centerpoint of the labyrinth and hence is not yet under the extreme transverse compression at the tip.

The transverse lines in the drawing represent cross sections which were mutually parallel and perpendicular to the medium centerline (shown dashed) in its undeflected state. It is well known from the mechanical behavior of materials that in pure bending these cross sections would be inclined to each other over the region of contact with the tooth tip, but remain parallel in the straight side wall. In the region of the tooth tip, the convex (outer) surface of the medium is stretched due to the bending and the concave (inner) surface adjacent to the tooth tip is compressed. The neutral surface (approximately the centerline) suffers no change in length due to bending.

As shown in Reference (17), the maximum strain due to bending is given by

$$\epsilon = \frac{t}{2R} = \frac{t/2}{r + t/2} \qquad (5)$$

where ϵ = maximum tension or compression strain, in./in.

t = caliper of medium, in.

R = radius of curvature of medium centerline, in.

r = radius of tooth tip, in.

This equation assumes that the medium is homogeneous and the tension and compression properties are identical. If the tensile load-elongation curve lies above the compression curve (tensile modulus of elasticity greater than the compressive modulus), the neutral surface of the bent medium will lie above the centerline in Fig. 19. In this event, the maximum tensile strain will be less than that given by Equation (5) and the maximum compression strain will be greater. Equation (5) is a consequence of the assumption that initially plane cross sections remain plane in bending--an assumption which has been accepted for strains beyond the limit of elasticity for many materials (18).

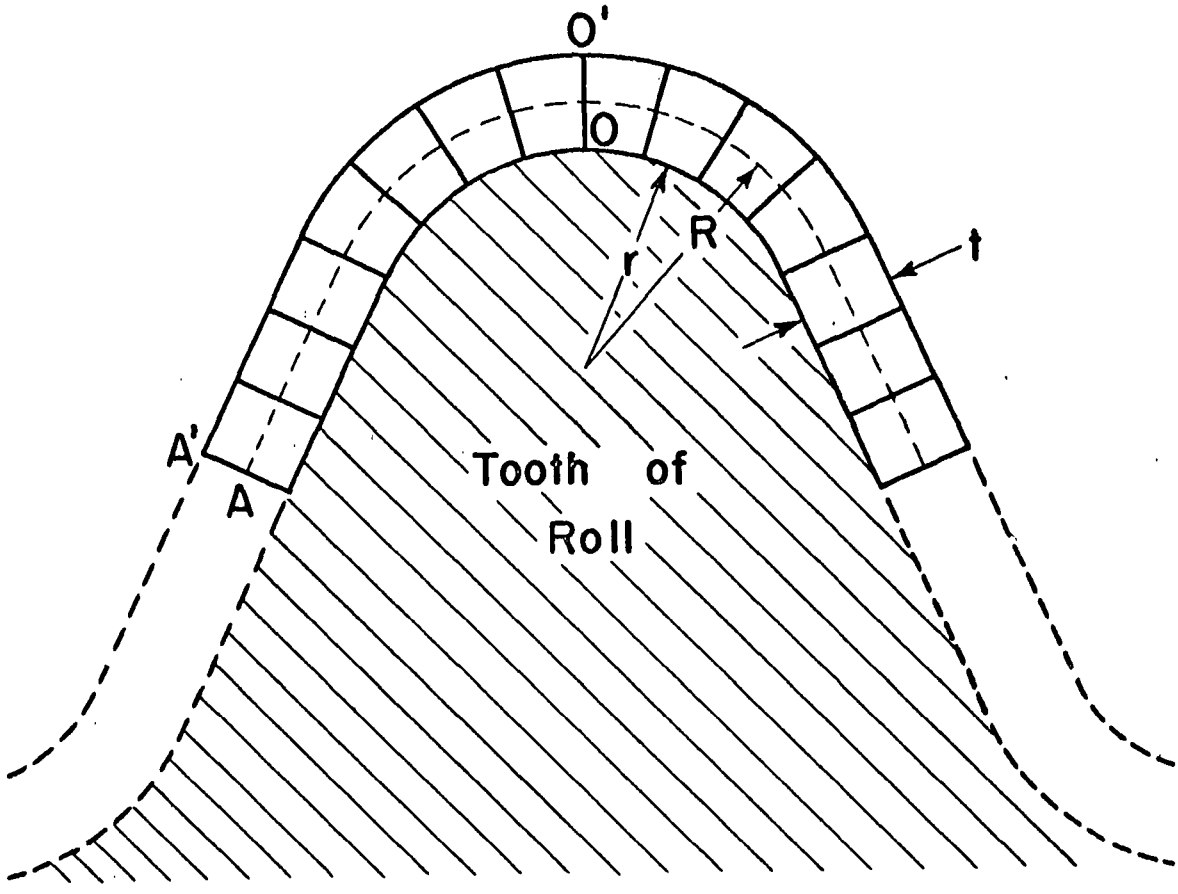

Fig. 19. Bending Deformation During Flute Molding

For the A-flute rolls studied here, the tip radius is $\underline{r}$ = 0.0582 in. For a medium of 0.010 in. caliper the calculated maximum bending strain around this tooth tip is:

$$\epsilon = \frac{0.010/2}{0.0582 + 0.010/2} = 0.08 \text{ in./in.} = 8\% \text{ for A-flute}$$

The tip radius of the B-flute teeth is 0.0490 in. Therefore, the bending strain is

$$\epsilon = \frac{0.010/2}{0.0490 + 0.010/2} = 0.093 \text{ in./in.} = 9.3\% \text{ for B-flute}$$

These are the strains which the medium must be able to withstand while being bent around the tooth tips if only pure bending is involved. Under this condition, bending induces tension strain on the convex side of the neutral surface of the medium which must be added to the transport tension strain, whereas on the concave side these strains are subtractive.

It is evident from Equation (5) that the maximum bending strain increases with caliper, $\underline{t}$. Thus, a thick medium would be expected to fracture more readily than a thin medium--all other conditions being equal. Furthermore, a small radius of curvature, $\underline{r}$, of the tooth tip also leads to high bending strains, as shown by the above numerical comparison of A- and B-flute. This observation indicates that the design of flute contours may need to be concerned with runability of the medium as well as performance of the fabricated combined board.

These induced bending strains (8 and 9%) seem to be unrealistically large in view of the fact that the available stretch of typical 26-lb. semi-chemical corrugating mediums in the machine direction at standard test conditions

is only about 1.5%. Furthermore, the stretch of the medium under the environmental conditions in the labyrinth may be markedly different from the stretch at standard conditions. The literature is practically void of information regarding the rheological behavior of paper or paperboard under the conditions encountered in the labyrinth. Anderson and Berkyto (19) have studied the stress-strain behavior of paper from 0 to 150°C. at 0 to 20% moisture. They found the tensile and stretch decreased with increase in temperature. It is well known that the stretch of paper decreases as the moisture content decreases. Trossett and Aiken (20) in a study of boxboard stiffness also found that in the temperature range of 70-100°F., the stiffness decreased with increase in temperature at a given relative humidity. Therefore, it would seem reasonable to expect that the medium would exhibit a much lower stretch (and possibly a lower modulus) under the conditions which are encountered in the labyrinth because of the elevated temperature and corresponding low moisture content of the medium at this point.

It is possible that the calculated strains may be erroneously high for two reasons: (a) the neutral surface may lie above the centerline due to the relative tension-compression characteristics of the medium, as discussed earlier [in this event, the distance from the neutral surface to the outer surface should be substituted in place of $t/2$ in Equation (5)]; (b) the small strain theory on which Equation (5) is based may not be appropriate to the large deflections of flute forming; severe bending may induce compressive stresses in the transverse (thickness) direction tending to reduce the caliper and thereby reduce the maximum tensile strain.

[It may be of interest to note that the bending strain at the smallest diameter idler roll (2-inch radius) is 0.25%, by Equation (5). This strain is less than the proportional limit strain of a typical medium in tension under a standard test environment and would not appear to be unrealistically high. The bending strain at the tensiometer roll (1.3-inch radius) is somewhat larger, namely, 0.38%.]

On the basis of the preceding comparison between bending strain and medium stretch, there is strong reason to suspect that bending of the medium to the tooth contour is accomplished by other types of strain than transport and pure bending. The most likely strain would appear to be shear strain. It is well known that shear strain accompanies bending strain in most conventional engineering structures of the flexure type. Frequently, the shear effects are so small that they may be neglected in engineering calculations. On the other hand, when the depth of a beam exceeds about 1/10 of the span, shear effects are no longer negligible (21). Each case must be judged on its own merits, of course, so it is appropriate that the effects of shear deformation be examined in connection with the flute-forming process.

The nature of shear strain as it may occur in flute molding is illustrated in Fig. 20. An element of material ABCD with sides of length dx is deformed into the parallelogram AB'C'D under the action of the shear stresses τ. The sides of the element suffer no change in length. The tangent of the shear angle ψ is defined (22) as the shear strain γ (i.e., $\gamma = \tan \psi$). For small angles ψ, the tangent of ψ is nearly equal to the angle ψ (in radians) so that the shear strain γ is essentially the angle of shear (23). As in the case of tensile or compressive strain, shear strain is dimensionless.

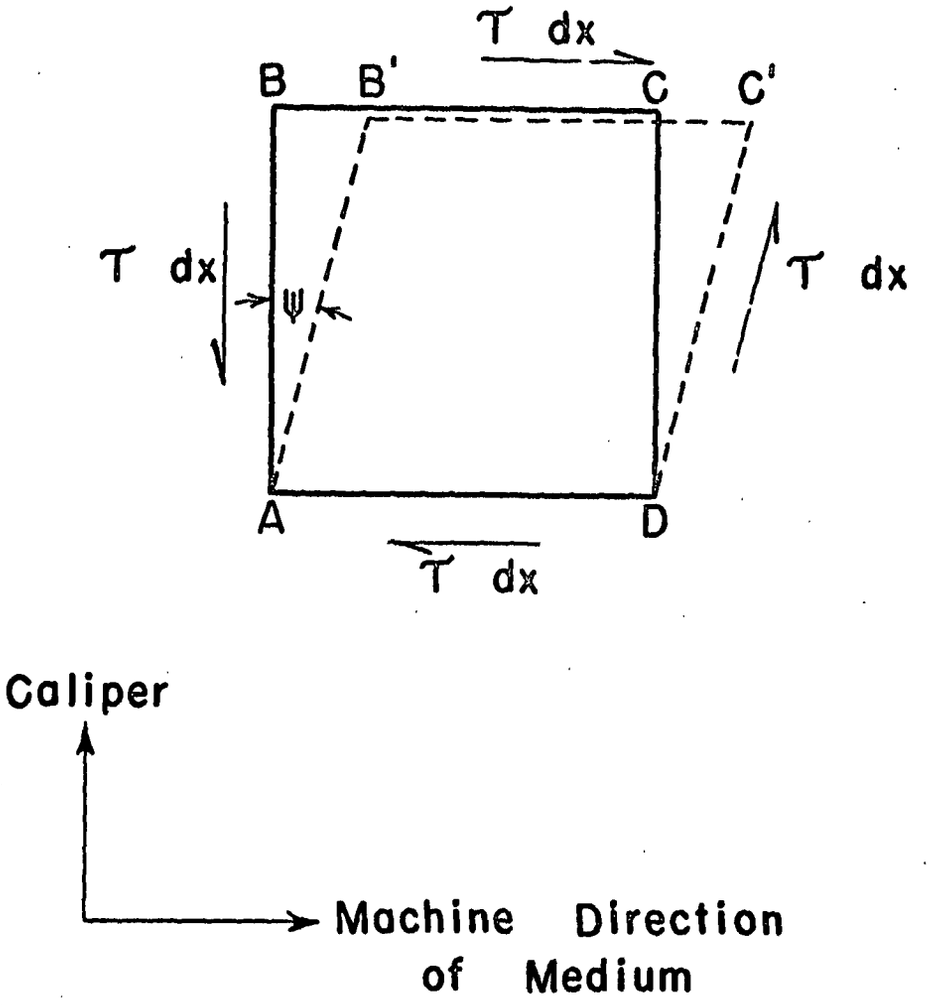

Fig. 20. Shear Strain

Figure 21 illustrates the portion of the medium shown previously in Fig. 19 as if all of the deflection were accomplished by shear strain (no bending taking place). As discussed in Reference (21), shear strain of the type pictured in Fig. 20 leads to the deformed cross sections shown in Fig. 21. The shear strain is maximum at the centerline of the medium and diminishes to zero at the outer surface because at that location normally there is no shear stress acting. This, of course, is in contrast to pure bending where the maximum strain occurs at the outer surface and reduces to zero strain approximately at the center of the medium. Thus, the deformed section remains perpendicular to the outer surface of the medium and the length ds remains unchanged from its original length before flute formation. The cross sections of Fig. 21 are drawn as though there is also no shear stress or strain acting at the surface of the medium which is in contact with the tooth. This assumption will be retained in the remainder of this discussion, although it should be recognized that the friction forces at the tooth may alter the shear deformation.

At any given instant, the shear strain in the medium at the apex of the tooth (point O, Fig. 21) must be zero by symmetry. Thus, the shear strain in the medium may be expected to be maximum at the mid-point of the side wall and decreases in absolute magnitude at an as yet unspecified rate until the tip of the tooth is reached, at which point the shear strain is zero.

Formation of the flute may be expected to be accomplished by a combination of bending and shear, that is, by a combination of the deformations pictured in Fig. 19 and 21. It may be noted that the presence of shear strain reduces the amount of bending strain which must be sustained in the medium in

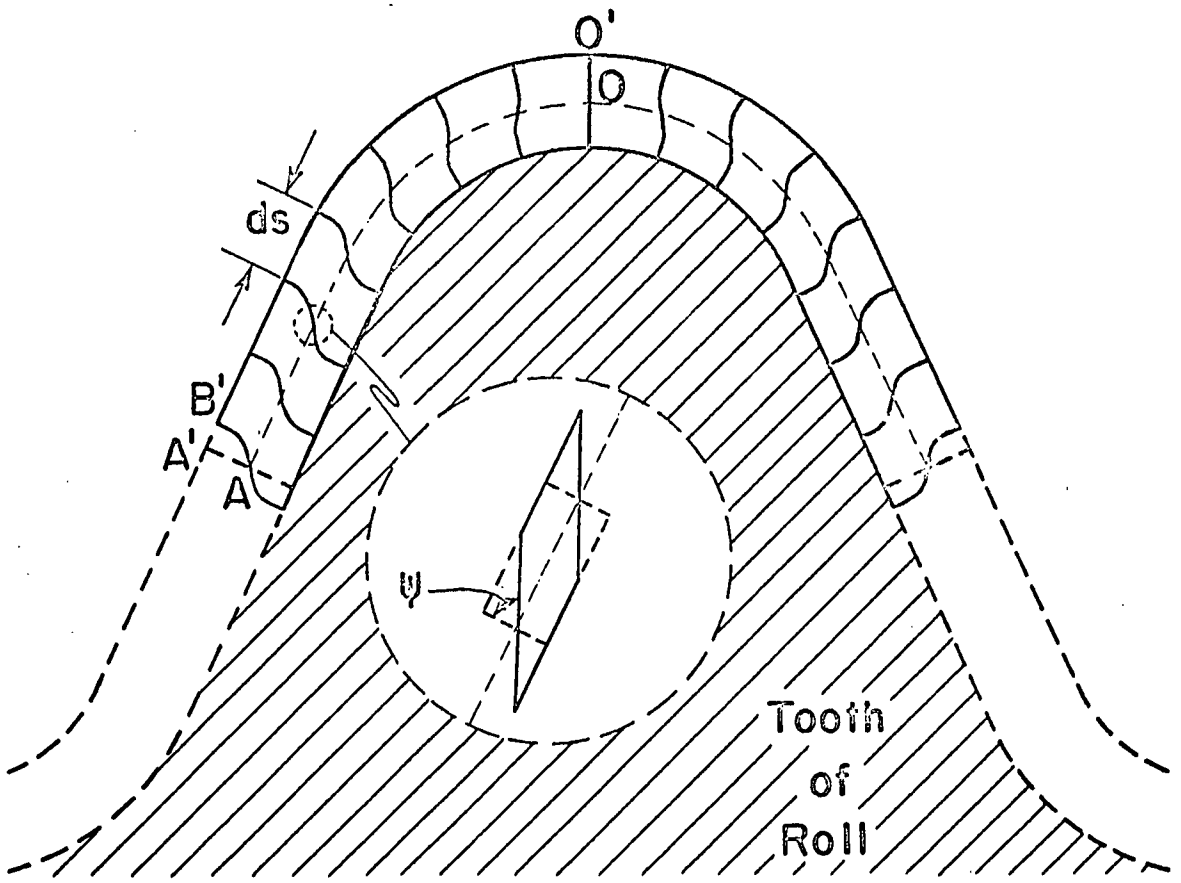

Fig. 21. Shear Deformation During Flute Molding

forming around the flute tip. This may be visualized in simplified terms as follows: If forming were accomplished solely by bending (see Fig. 19), the total tensile elongation at the outer surface would be the difference in arc lengths of the curves OA and O'A'. Because of the shear displacement A'B' of Fig. 21, however, the tensile elongation due to bending, e, need be only:

$$e = (O'A' - OA) - A'B'$$

That is, shear deformation reduces the apparent bending deformation by the amount A'B'. This explanation, however, is phrased in terms of total elongation and does not speak to the pertinent point of how the bending strains and shear strains are distributed along the length of the medium under consideration.

It may be expected that the bending and shear strains will apportion themselves according to the stiffnesses of the medium with respect to these two types of deformation. For example, if the material is relatively stiff in shear compared to its stiffness in bending, the deformations induced in forming the medium to the contour of the tooth will be predominantly bending strains (as occurs with many metallic structures). On the other hand, if the material is relatively stiffer in bending than in shear, then the medium will find it easier to form by means of shear strains than by bending strains. Exact analysis of the division between shear and bending strains is a difficult problem. Ultimately its solution demands giving attention to the stress accompanying the strain (the two are related by the stiffness factor of the medium) and thereby finding a distribution of stresses which are compatible with the forces applied externally to the medium. This is the crux of the

corrugating operation and the solution of this problem must be obtained if corrugating is to be adequately described from the mechanics of materials standpoint.

For the purpose of gaining a better insight into the flute-forming process an approximate analysis of flute-forming strains is given in this report. The derivation is presented in Appendix B and only the discussion of results is treated herein.

In the approximate analysis, a plausible distribution of bending and shear strain is assumed. It is assumed that bending is restricted to the portion of the medium pictured in Fig. 19 which lies in contact with the circular arc of the tooth tip. Furthermore, it is assumed that the bending strain, ϵ, at the extreme fibers of the medium is constant along this arc. On the other hand, the shear strain at the medium centerline is assumed to be constant over the side wall of the flute (i.e., the portion of the flute which is straight) and is equal to γ_w (= tan ψ_w). In addition, it is assumed that the shear strain, diminishes linearly with distance along the circular arc, reaching zero at the apex of the flute.

For these assumed distributions of strain, the strain analysis presented in Appendix B yields a relationship between the magnitudes of shear and bending strain which satisfy the geometrical requirements of flute forming. A graphical presentation of this relationship is given in Fig. 22 for A- and B-flute contours. Both curves are straight lines. The co-ordinates of a point on either curve represents one combination of shear angle, ψ_w, and bending strain, ϵ, which will permit a medium of

0.010-inch caliper to assume the fluted shape at a point in the labyrinth one tooth ahead of the centerpoint. For example, point x represents one combination of strains which would satisfy the geometrical requirements of bending the medium into an A-flute contour of the dimensions considered in this study. At this point (x), the bending strain, ϵ, equals 0.03 in./in. and the shear angle, ψ_w, equals 0.7 radian. The case of all bending and no shear is represented by point b on the horizontal axis, namely $\epsilon = 0.08$ in./in., while the case of all shear and no bending is given by the intercept s on the vertical axis, 1.15 radian.

It should be emphasized that the curves of Fig. 22 are derived solely from geometrical considerations and do not account for the physical properties of the medium in shear and bending. The curves depend only on the tooth contour and the caliper of the medium (0.010 inch in this case). Distinctly different strain curves would be applicable to mediums of different caliper. To the accuracy of the theory employed, a curve of Fig. 22 defines all possible combinations of bending and shear strains which would permit a medium of 0.010-inch caliper to be formed into a flute of the dimensions used in this study.

The data of Fig. 22 should be considered as illustrative rather than actual values of the bending and shear strain. As discussed in greater detail in Appendix B, small deflection theory has been utilized in this analysis to describe what is undoubtedly large deflection behavior. Accordingly, several of the assumptions and techniques employed in the analysis are questionable. Among these are: (a) method of superposition

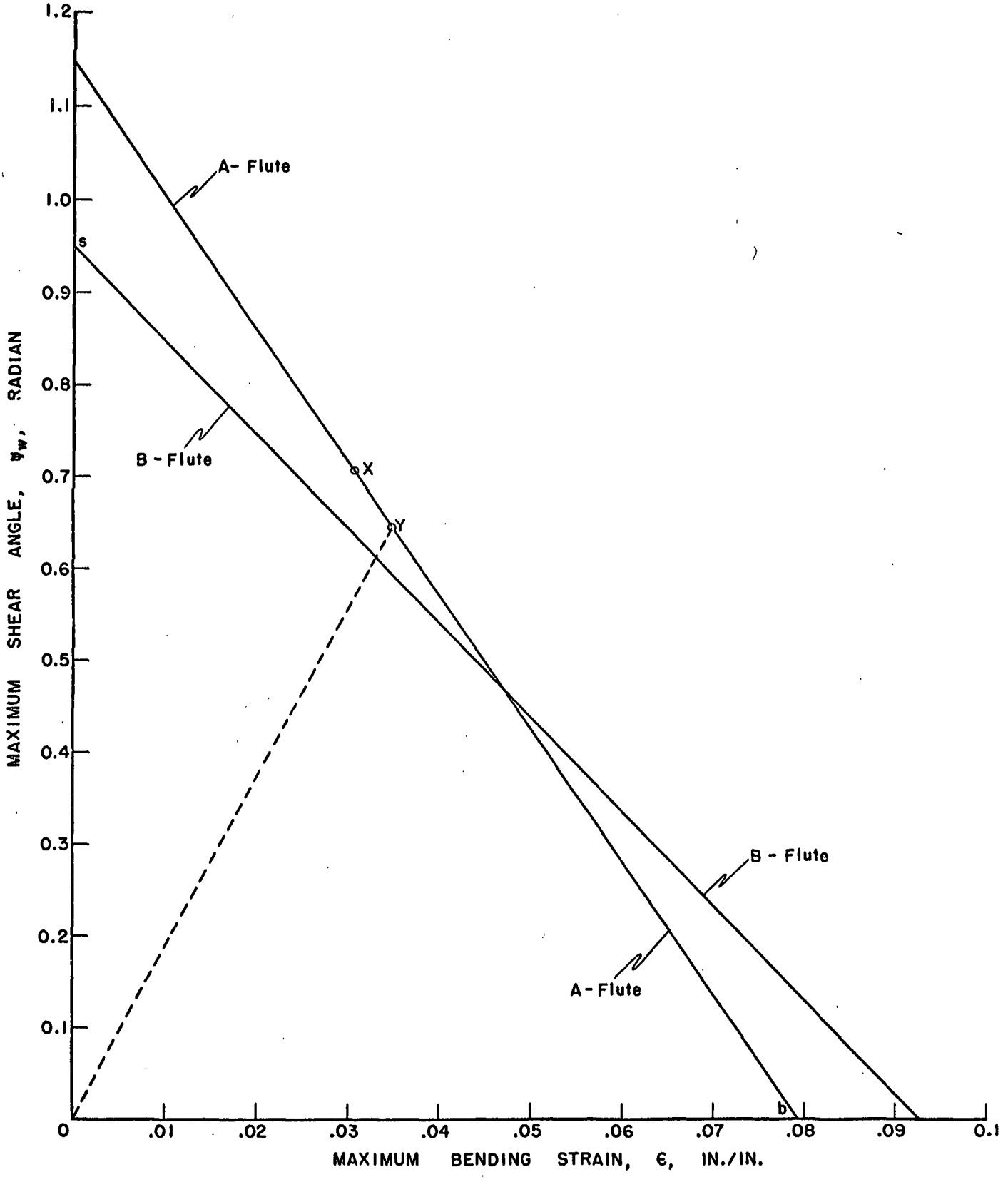

Fig. 22. Relationship Between Bending and Shear Strain Required for Flute Molding (Based on Small Deflection Theory)

of bending and shear curvatures; (b) the distribution of shear and bending strains across the caliper of the medium; (c) no reduction in caliper; (d) zero strain axis at the medium centerline, and (e) absence of shear stress at the medium surface adjacent to the tooth tip, and (f) medium is sufficiently homogeneous to be treated as a conventional engineering material. It is believed that a consequence of (a) through (c), if they are in error, will be an overestimation of strains. The shear angles of Fig. 22 appear to be exceedingly large; 0.7 radian is approximately 40°. Moreover, it is likely that a more exact analysis of the forming strains will lead to strain curves other than straight lines shown in Fig. 22.

Nonetheless, the curves of Fig. 22 are believed to illustrate the principles involved in bending the medium to the contour of the tooth. It may be seen that if the bending strain is to be small, the shear strain must be large to permit forming of the flute, and vice versa. This analysis does not determine, however, which combination of shear and bending strains is induced in a given medium under given corrugating conditions. The particular combination obviously depends on the relative properties of the medium in shear and bending. More specifically, the apportionment of shear and bending may be expected to depend on the inelastic equivalent of the ratio

$$\frac{EI}{GA}$$

where E = modulus of elasticity, lb./in.^{2}

I = moment of inertia of medium cross section, in.^{4}

G = shear modulus, lb./in.^{2}

A = area of cross section, in.^{2}

The inelastic equivalent of E is the slope of a line from the origin to the point on the stress-strain curve corresponding to the level of stress or strain induced in the medium, and analogously for the inelastic shear modulus. Changes may also occur in A and I due to change in caliper. It should be recognized that the inelastic equivalents of E and G are dependent on the respective strain levels, so that the inelastic equivalent of the stiffness ratio, EI/GA, is itself a function of the strains. Speaking in broad terms, however, it may be reasoned that if the stiffness ratio is generally large throughout the inelastic portions of the stress-strain curves, forming will be predominantly shear strain--corresponding to the upper left portion of the curve of Fig. 22. If the ratio is generally low, forming will be largely bending strain--the lower right portion of the strain curve of Fig. 22.

Inasmuch as the moment of inertia, I, depends on the cube of the caliper, t, and the cross-section area depends on the first power of caliper, the ratio I/A increases with caliper. All other factors being equal, an increase in caliper may be expected to increase the stiffness ratio and thereby increase the proportion of shear strain relative to bending strain, even though both strains increase.

In view of the preceding discussion of apportionment of bending and shear strains, it is conceivable that corrugating mediums may exhibit differing proportions of shear and bending strain, as a result of differences in E, G and caliper.

One way of interpreting the curves of Fig. 22 is as follows: For a given ratio of material properties in shear and bending, the shear and

bending strains may be expected to build up from zero along some dashed curve such as $\overline{OY}$ in Fig. 22 as the flute is being formed. It is not necessary that this dashed curve be a straight line as pictured; rather, it may be expected to be a function of the shape of stress-strain curves of the medium in shear and tension and compression. The intersection point, Y, of the dashed curve and the A-flute curve of Fig. 22 denotes the strains which the medium must be capable of sustaining without rupture if the medium is to be corrugated successfully. For this illustration, the medium must have an available stretch in excess of 3.5% in the machine direction and an allowable shear angle in excess of 0.65 radian. If the medium "strength" is less than these values, it may be expected to rupture according to whichever type of critical strain was exceeded during corrugation. A bending failure may manifest itself as a rupture of the extreme outer surface fibers, since this is the location of greatest strain (the strain due to transport tension is additive to bending strain). On the other hand, a shear rupture would manifest itself as a delamination of the medium at the point where the critical shear strain is reached, normally along the centerline of the medium. When delamination takes place the strain in the extreme fiber layer due to bending is reduced and therefore no rupture of the surface fibers would be expected.

It is not a foregone conclusion, however, that medium rupture must necessarily occur at either the surface or at the center of the medium. If one appeals to the experience gained with other orthotropic materials, it may be expected that the strength of the medium under the action of combined tension and shear may be expected to be less than its strength under either

stress acting separately. This concept is illustrated graphically in Fig. 23, which is an adaptation of the theory presented in Reference (24). The curve of Fig. 23 is known as an interaction curve, any point of which describes the magnitude of tensile stress and shear stress which in combination cause rupture of the material. Point T denotes the tensile strength when no other stresses are acting, and similarly point S denotes the shear strength when only shear is present. A point such as Z, on the other hand, reveals that failure will occur under the combined action of a tensile stress and a shear stress which are less than their respective ultimate strengths.

Conceivably, rupture may occur in a medium under the conditions depicted by point Z, for the following reason. Figure 24 illustrated the distribution of bending and shear strains acting on a cross section of the fluted medium of caliper t according to the small deflection theory employed in Appendix B. The vectors of Fig. 24(a) denote the intensity of tensile and compression strains. The maximum tensile strain is larger than the maximum compressive strain because of the added uniform strain due to transport tension. The ordinates to the curve of Fig. 24(b) depict the intensity of shear strain---a parabolic variation from a maximum at the centerline to zero at the inner and outer surfaces. It is conceivable that the stresses at some point which is a distance y from the centerline may yield a critical combination such as the point Z on the interaction curve of Fig. 23, whereupon rupture would be expected to initiate at that point on the cross section rather than at the surfaces or at the centerline. It is not evident at this time as to the exact appearance of this type of rupture.

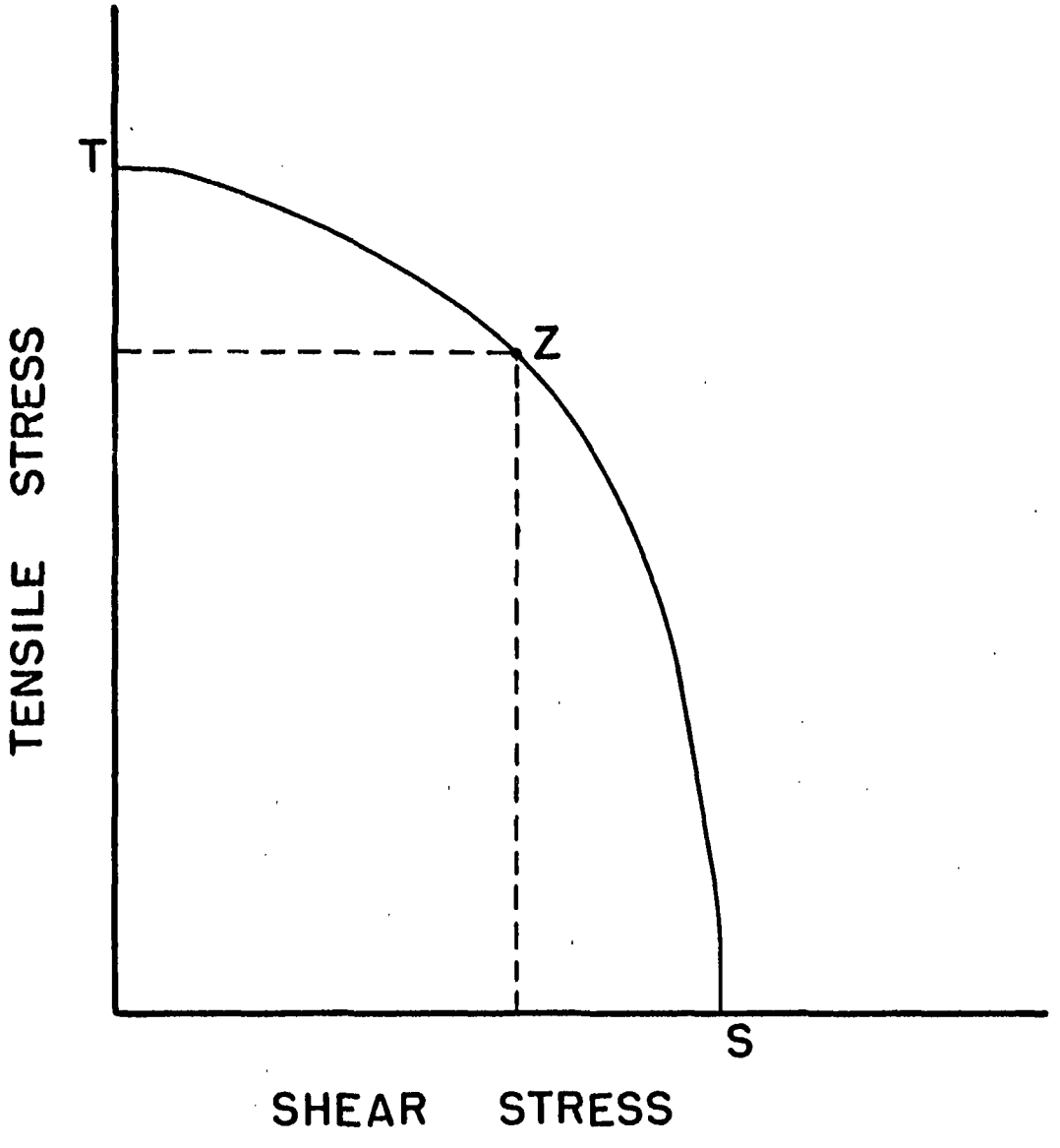

Fig. 23. Theoretical Interaction Curve of Failure of Medium Due to Combined Tension and Shear

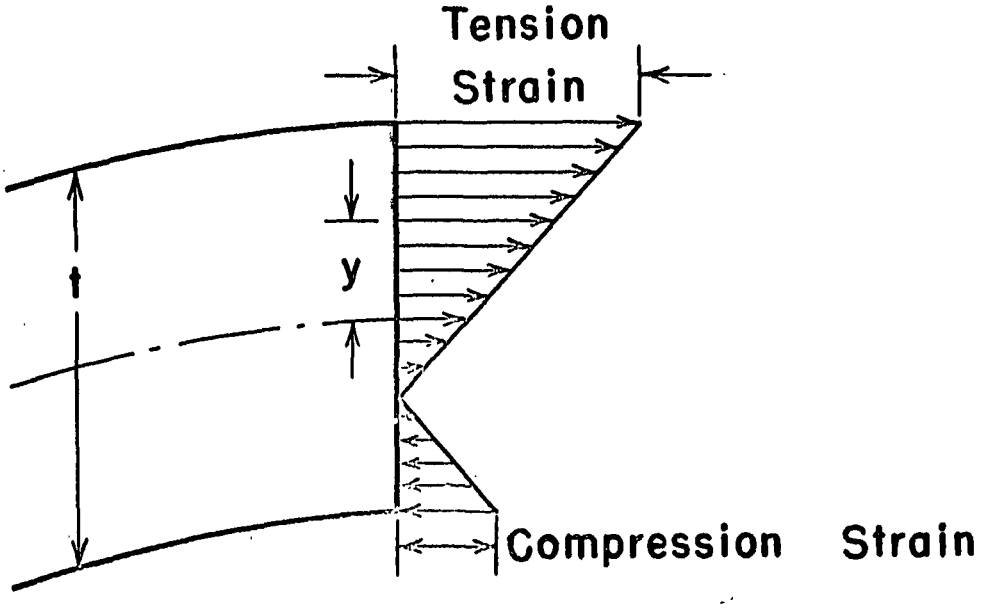

(a) Bending Strain

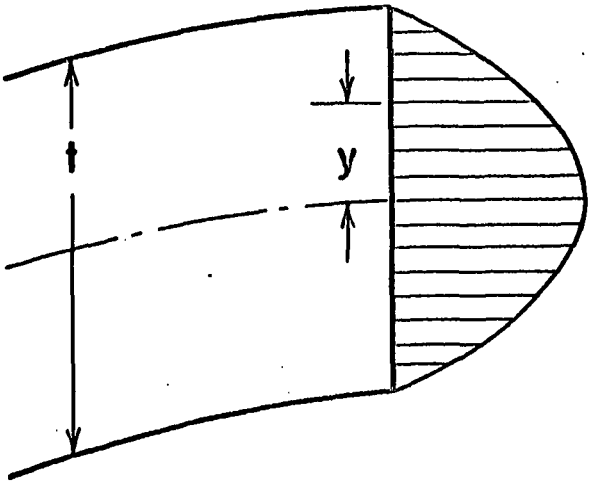

(b) Shear Strain

Fig. 24. Distribution of Bending and Shear Strain on Medium Cross Section

(Based on Small Deflection Theory)

In view of the assumed distribution of bending and shear strains along the medium (in contrast to distribution across the caliper), one may expect that rupture of the medium would occur at the junction of the side-wall and the circular tip portion. This is the point of apparent maximum shear and bending strains. The occurrence of rupture at this location has been verified in limited number of high-speed motion pictures of medium during corrugating. Rupture reveals itself as a flare in the film, due to a change in light reflectance as the fibers rupture. The fracture has been observed to take place at the junctions on the left side of teeth F and E in Fig. 9. It was not possible, however, to ascertain where on the cross section the rupture initiated, for lack of sufficient magnification.

Returning to Fig. 22, it may be noted that the strain curve for B-flute crosses over the A-flute curve at $\epsilon = 0.045$ in./in. The relative orientation of the A- and B-flute curves may be explained in terms of tooth contours. If the forming of the medium to the contour of the tooth is accomplished primarily by bending strain, the lower right hand portion of the curves indicate the relative proportions of the strains involved. In this region, the higher bending strain for B-flute is attributable to the smaller radius of curvature of the tooth--0.0490 in. vs. 0.0582 in. for the A-tooth. On this basis B-flute would be more susceptible to fracturing than A-flute under the same corrugating conditions.

On the other hand, if shear is the predominant forming strain, the upper left portion of the curves describes forming. As shown in Appendix B, the shear strain is largely dependent on the slope of the flute side wall. Since the B-flute has a smaller side-wall angle than the A-flute (54.5° vs. 66°,

measured from a line parallel to the width dimension of the flute), the B-flute would be expected to incur the lower shear strain. Under these conditions B-flute would be less susceptible to fracturing than A-flute. It is generally observed in commercial practice that B-flute is less susceptible to fracturing than A-flute. While this behavior may be attributable to greater friction for A-flute, as discussed earlier in this report, it may also be an indication that the forming strains are apportioned in accordance with the curves lying to the left of the intersection point of Fig. 22. This may be interpreted as indicating that relatively large shear strains are involved in forming in addition to bending strains.

In summary, analysis of stresses and strains suggests that formation of the flute involves severe deformations of the medium as it attains the contour of the roll tooth. These deformations are apparently a combination of shear strain and bending strain, apportioned according to the ratio of bending stiffness and shear stiffness of the medium in the range of inelastic strains. If the medium has insufficient stretch or insufficient allowable shear strain to meet the geometrical requirements of forming around the tooth tip, fracture of the medium may be expected to occur as the flute approaches complete formation about one to two teeth ahead of the line joining the centers of the corrugating rolls.

RELATIONSHIP BETWEEN RUNABILITY AND STRESS-STRAIN STATE IN MEDIUM

It may be noted that the foregoing analyses of stress and strain in the medium during corrugating contained no explicit factor involving corrugating speed. The sole exception was centrifugal tension which was negligibly small even at a corrugating speed of 1000 ft./min. Runability is measured in terms of corrugating speed and for each medium there is a limiting speed beyond which the medium will fracture. Thus, an adequate stress-strain analysis of corrugating must account for the effects of corrugating speed.

It should be mentioned that corrugating speed enters indirectly into several of the types of stress and strain to which the medium is subjected during corrugating. In considering these effects it may be helpful to distinguish between (a) induced strain and (b) allowable strain which the medium is capable of withstanding, i.e., its stretch and allowable shear strain.

With regard to induced strain, it may be recalled that the transport tension in the medium is in part dependent on the coefficient of kinetic friction between the medium and the heated corrugating rolls--the greater the coefficient of friction, the greater is the force of friction and hence the greater is the transport tension. Work at The Institute of Paper Chemistry (15) indicates that the coefficient of friction of a variety of commercial mediums under standard test atmosphere were sensibly independent of speed in the speed range of 50 to 200 ft./min. On the other hand, an increase in corrugating speed probably decreases the temperature and increases the moisture content of the medium because of the more rapid passage of the

medium through the corrugator. In connection with the previously cited work (15), it was also found that the coefficient of friction (a) increased with decrease in temperature, and (b) increased with increase in moisture content. Thus, the changes in temperature and moisture content of the medium, associated with increase in corrugating speed, may be expected to increase the force of friction and hence the transport tension induced in the medium. This is analogous to increasing the initial web tension, T_o. It has been shown that runability is inversely related to web tension (9).

Secondly, it seems intuitive that increases in corrugating speed will result in greater impact forces on the medium as it enters the labyrinth, leading therefore to an increase in transport tension as the medium enters the forming stage. This conjecture is not necessarily at variance with the oscilloscopic record from the tensiometer, reproduced in Fig. 16. The observation that the fluctuating trace--believed to be the impact stress from the first tooth of the labyrinth--shows no progressive increase with corrugating speed may be due to insufficient response of the tensiometer.

The final shape of the flute at the center of the labyrinth is, of course, determined by the tooth contour and not by the speed of corrugating. On the other hand, the apportionment of strains between bending and shear during flute formation may depend on the corrugating speed for the following reason. The strain apportionment is believed to be dependent on the relative stiffness of the medium in bending and shear--that is, the inelastic equivament of EI/GA. The moduli in bending, E, and shear, G, are functions of the stress-strain curves of the medium with respect to these two types of strain. It has been shown (11, 19, 25) that the tensile modulus of elasticity of paper

increases with decrease in temperature, decrease in moisture, and increase in rate of straining. It should be emphasized that although tensile strength follows the same trend as the modulus, the stretch does not. For example, the stretch increases as the temperature decreases and as the moisture content increases, but stretch decreases as the rate of straining increases. It seems reasonable to expect shear and compression properties to follow the same trends. It is conceivable, therefore, that the inelastic equivalent of the ratio $\underline{E}/\underline{G}$ may change with increase in corrugating speed and thus cause a different apportionment of shear strain and bending strain; for example, the bending strain may increase and the shear strain may decrease relative to their values at a lesser corrugating speed. The increase in speed may therefore cause one of the induced strains to exceed the allowable strain of the material whereas it did not at the lower speed.

Thus, with regard to induced strain, it may be anticipated that with a given medium an increase in corrugating speed may increase transport tension (increase in $\underline{u}$ and impact) and cause a reapportionment of bending and shear strains.

Turning now to the allowable strain which the material can withstand, it appears likely that the increased rate of straining accompanying increases in corrugating speed will decrease the stretch and allowable shear strain of the medium. This effect has been demonstrated in the case of stretch (11, 25) and may be expected to occur in the case of shear also. An increase in corrugating speed may decrease the temperature and increase the moisture content of the sheet, as mentioned above. Based on the work of Reference (19), both the decreased temperature and increased

moisture content may be expected to result in an increase in the allowable strain of the medium. Thus, the effect of increase in speed on temperature and moisture content of the medium may tend to compensate for the loss in allowable strain associated with the higher rate of straining. It is not clear at this time, therefore, what may be the net effect of speed on the strains which the medium can safely withstand.

In summary, it is anticipated that an increase in corrugating speed may change both the strain induced in the medium during corrugating and also the allowable strain which the medium can sustain. It appears likely that the transport tension will increase and that the apportionment of forming strain between bending and shear will be altered when the corrugating speed is increased. It is not evident, however, whether the allowable strains of the medium will increase or decrease, because of compensating effects associated with rate of straining vs. temperature and moisture content.

The following combinations of the above-mentioned effects would be conducive to rupture of the medium as a result of increased corrugating speed:

Case I. Increase in induced strain and decrease in allowable strain.
Case II. Increase in induced strain and no change in allowable strain.
Case III. A greater increase in induced strain than in allowable strain.
Case IV. A greater decrease in allowable strain than in the induced strain.

In considering the physical properties of the medium, attention perhaps should be given to the fatigue of paper and paperboard. The medium

is repeatedly stressed as it approaches the labyrinth due to the impacts of the first tooth of the labyrinth. In the classical sense (26) fatigue failure occurs as a result of a large number of repeated applications of a given or varying level of stress--the greater the applied stress, the fewer replications the material can withstand before rupture. In the case of paper, it is believed that repeated applications of sufficiently high stresses may deteriorate the strength of the medium, thereby reducing the allowable strains determined from environmental tests which account for only heat, moisture, and rate of straining. This belief stems from consideration of the rheological behavior of paper as reported, for example, in Reference (11).

Fatigue behavior (in either the classical sense or the rheological sense) involves two primary factors: (a) the intensity of the applied stress, and (b) the number of times the stress is applied, that is, the number of cycles of stress. It may be reasoned that it is the stress intensity aspect of fatigue rather than the number of cycles which may be directly associated with runability--that is, runability in the sense of a limiting corrugating speed--for the following reason: There may be assumed to be some point in the web ahead of the labyrinth where the magnitude of impact stress is diminished to the point of being negligible. For the sake of illustration, let this point be 156 inches ahead of the labyrinth. At a corrugating speed of 500 ft./min., the frequency of impact stress is 300 cycles/second (corresponding to the rate of flute formation) and the web travels at a speed of 156 inches/second. Thus, a given element of medium requires one second to travel from the point of assumed negligible impact to the entrance of

the labyrinth. During this second the element receives 300 cycles of impact stress. The intensity of the stress on the element may be expected to increase as the element approaches the labyrinth.

Now suppose the corrugating speed is doubled, from 500 to 1000 ft./min., whereupon the web speed is 312 inches/second and the impact frequency is 600 cycles/second. The given element now reaches the labyrinth in one-half second, during which time it receives 600/2 = 300 impacts, the same number as before. This type of argument evidently applies to any element of medium in the web. Thus, increasing the corrugating speed does not increase the number of the impacts received by an element of medium.

On the other hand, the magnitude of the impact probably increases with speed (as well as with location on the web) as discussed earlier, so that 300 impacts (to cite the example above) of increasing level of stress may deteriorate the medium sufficiently to cause failure at the forming stage. Thus, determination of allowable strains of the medium might reasonably include fatigue as an environmental condition in addition to heat, moisture, and rate of straining.

LITERATURE CITED

1. Werner, A. W. Contemporary flute design. Tappi 36, no. 5:167-70A (May, 1953); Fibre Containers 38, no. 3:64, 66, 68 (March, 1953--abridgment).

2. Wilson, H. W. How and why flute contour affects corrugated quality. Fibre Containers 40, no. 11:69, 73—5 (Nov., 1955).

3. Ward, W. F. Design of new single-facer. Fibre Containers 40, no. 3: 52-60 (March, 1955).

4. Wilson, H. W. An operator's thought on flute contour. Tappi 39, no. 7: 146-8A (July, 1956).

5. Nitchie, C. D. Flute contour studies. Fibre Containers 42, no. 4:50-2, 71 (April, 1957).

6. Wilson, H. W. W-S flute desigh brings new concept of corrugating. Fibre Containers 44, no. 4:69-72 (April, 1959).

7. Spaulding, R. O., and Wallis, S. W. Owens-Illinois develops new C-flute contour. Fibre Containers 44, no. 6:44-6 (June, 1959).

8. Goetsch, W. M. Adhesive application on the single-facer and double-backer. Tappi 39, no. 7:143-5A (July, 1956).

9. McKee, R. C. Corrugating variables and the effect on combined board performance. Presented at Fall TAPPI Corrugating Conference, New Orleans (Sept. 16, 1959).

10. McKee, R. C. New corrugator broadens Institute research. Fibre Containers 44, no. 2:58-60 (Feb., 1959).

11. Steenberg, Börje. Behaviour of paper under stress and strain. Pulp Paper Mag. Can. 50, no. 3:207-14, 220 (1949).

12. Marks, L. C. Mechanical engineers' handbook (textbook edition) p. 205. New York, McGraw-Hill Book Co., 1951.

13. Reference (12), p. 142.

14. Reference (12), p. 228.

15. The Institute of Paper Chemistry, unpublished data.

16. Oil mist lubrication of single facer improves corrugated board production. Paper Trade J., 138, no. 20:134 (May 14, 1954).

17. Timoshenko, S. Strength of materials, Part I. Elementary theory and problems. New York. D. van Nostrand Co., 1955. p. 93.

18. Nadai, A. Theory of flow and fracture of solids. New York. McGraw-Hill Book Co., 1950. p. 353.

19. Andersson, O., and Berkyto, E. Some factors affecting the stress-strain characteristics of paper. Svensk Papperstidn. 154, no. 13:437-44 (July 15, 1951).

20. Trossett, S. W., and Aiken, W. H. A study of some information which affect the stiffness of folding boxboard. Tappi 41, no. 3:177A-86A (March, 1958).

21. References (17), p. 118, 170.

22. Reference (18), p. 120.

23. Reference (17), p. 59.

24. Norris, C. B. Strength of orthotropic materials subjected to combined stresses, USDA Forest Service, Forest Products Laboratory, Madison, Wis., Report No. 1816, July, 1950.

25. Nissan, A. H. The rheological properties of cellulose sheets: Retrospect and synthesis. Tappi 39, no. 2:93-7 (Feb., 1956).

26. Reference (12), p. 402.

27. Reference (17), p. 138.

THE INSTITUTE OF PAPER CHEMISTRY

James W. Gander

James W. Gander, Research Aide,
Container Section

R C McKee

R. C. McKee, Chief, Container Section

APPENDIX A

ANALYSIS OF FRICTION ON CORRUGATOR ROLLS

The following tables list data pertinent to the accumulation of friction on the top corrugating roll and in the labyrinth for A- and B-flute contours. In each table the columns pertain to six angular portions of the corrugating rolls, denoted by the distance of a tooth tip of the lower roll from the centerpoint of the labyrinth during formation of one flute. The first line of data is the angle of contact at the first tooth where the medium enters tangentially onto the top corrugating roll; it is numerically one-half of the flute angle--that is, the angle subtended at the center of the roll by one tooth.

The second line of data is the sum of contact angles over the remaining teeth of the top roll prior to the beginning of the labyrinth. Each angle of contact in this sum is equal to the flute angle. The following four or five lines are the contact angles at individual teeth in the labyrinth up to the tooth of estimated zero-slip. The following two lines in the table are the sum of all the contact angles, expressed in degrees and in radians.

The remaining lines of the table are calculated values of the ratio

$$T_m/T_o = e^{\mu \Sigma \beta}$$

for various values of μ. In both flute analyses the maximum value of the ratio occurred at the position denoted "3/4" and is so indicated at the foot of the column.

TABLE III

CALCULATION OF TENSION DUE TO FRICTION IN A-FLUTE LABYRINTH ($T_m/T_o = e^{\mu\Sigma\beta}$)

	Position, Fraction of Flute Width from Centerpoint					
	0	1/8	1/4	3/8	1/2	3/4
Initial β, degree	1.64	1.64	1.64	1.64	1.64	1.64
Σ β outside labyrinth, degree	42.51	42.51	42.51	42.51	42.51	42.51
β inside labyrinth, degree	11.5	6.5	41.5	37.0	32.0	18.5
	18.0	7.5	77.5	68.0	59.5	40.0
	59.0	49.5	104.0	98.5	92.0	79.0
	92.0	85.5	120.5	118.0	114.0	106.0
	113.0	109.5				121.0
Σβ, degree	337.65	302.65	387.65	365.65	341.65	408.65
Σβ, radian	5.89	5.28	6.77	6.38	5.96	7.13
μ= 0.10, $e^{\mu\Sigma\beta}$ =	1.80	1.70	1.97	1.89	1.82	2.04
0.15,	2.42	2.21	2.76	2.60	2.45	2.92
0.20,	3.25	2.88	3.87	3.58	3.30	4.16
0.25,	4.36	3.75	5.43	4.93	4.44	5.95
0.30,	5.86	4.88	7.61	6.78	5.98	8.50
0.35,	7.87	6.35	10.68	9.33	8.06	12.14
0.40	10.56	8.27	14.97	12.84	10.86	17.34
						Maximum

TABLE IV

CALCULATION OF TENSION DUE TO FRICTION IN B-FLUTE LABYRINTH ($T_m/T_o = e^{\mu \Sigma \beta}$)

	Position, Fraction of Flute Width from Centerpoint					
	0	1/8	1/4	3/8	1/2	3/4
Initial β, degrees	1.15	1.15	1.15	1.15	1.15	1.15
Σβ outside labyrinth degree	46.20	46.20	48.51	48.51	48.51	46.20
β inside labyrinth degree	8.0	6.5	31.5	27.5	23.0	16.0
	13.5	8.0	61.0	54.0	46.0	29.5
	43.5	39.0	88.5	81.5	75.0	59.0
	70.5	69.0	107.0	103.0	97.5	85.5
	94.0	92.5				105.0
Σβ, degree	276.85	262.35	337.66	315.66	291.16	342.35
Σβ, radian	4.83	4.58	5.89	5.51	5.08	5.98
μ = 0.10, $e^{\mu \Sigma \beta}$ =	1.62	1.58	1.80	1.74	1.66	1.81
0.15,	2.06	1.99	2.42	2.28	2.14	2.44
0.20,	2.63	2.50	3.25	3.01	2.76	3.29
0.25,	3.35	3.14	4.36	3.96	3.56	4.43
0.30,	4.26	3.95	5.86	5.22	4.59	5.97
0.35,	5.43	4.96	7.87	6.88	5.92	8.04
0.40,	6.91	6.24	10.56	9.06	7.63	10.84
						Maximum

APPENDIX B

ANALYSIS OF BENDING AND SHEAR STRAINS DURING FLUTE FORMING

Forming of the medium around a tooth tip may be expected to be accomplished by a combination of bending strain and shearing strain in the medium. It will be assumed for purposes of this discussion that the total deflection, y_t, of the medium from its initially straight form to its final formed shape may be taken as a superposition of its deflection, y_b, due to bending and its deflection, y_s, due to shear.

The deflection y_b of a portion of the flute due to bending strain is pictured in Fig. 25. Under solely bending action, plane cross sections of the flute remain plane; hence, a rectangular element of initial length ds is deformed into a rhombus, such that the fibers on the convex side of the beam are lengthened (tensile strain) and fibers on the concave side are shortened (compression strain). An element of length near the mid-plane of the beam will suffer no change in length (called the neutral surface) and hence is unstrained and unstressed. The location of the neutral surface depends on the tensile and compression characteristics of the material. If tensile and compression properties are equal (in a bent member of rectangular cross section) the neutral surface lies at the mid-plane of the beam. It will be assumed in the remainder of this analysis that the neutral surface is at this position.

It is shown in Reference (27) that the curvature (i.e., the reciprocal of the radius of curvature R_b) is given by

$$\text{Bending curvature} = \frac{1}{R_b} = \frac{d\,\theta_b}{d\,s} \qquad (6)$$

where R_b = radius of curvature due to bending, in.$^{-1}$

θ_b = angle between tangent line of curve and x-axis, radian

s = co-ordinate of length along the beam, in.

(In the case of very small deflections $\theta_b \doteq dy/dx$ and $ds \doteq dx$, whereupon Equation (6) becomes $1/R_b = d^2y_b/dx^2$, the familiar approximation for curvature). It is also shown in Reference (17) that the maximum unit strain, ϵ, at the extreme fibers due to bending is

$$\epsilon = \frac{t}{2 R_b} \qquad (7)$$

where ϵ = maximum tension (or compressive) strain, in./in.

t = caliper, in.

Equation (7) is a consequence of the assumption that plane sections remain plane in bending, that is, the strain ϵ is proportional to the distance of the fiber in question from the neutral surface.

Figure 26 shows the deflection of a portion of a beam due to shear strain. Here, an initially plane cross section a-a (shown by a dashed line) is deformed into the curved cross section b-b. The angle $\overline{a0c}$ is the shear angle, ψ, at the centerline. The shear strain, γ, is defined as the tangent of the angle ψ, (22). For small angles, $\gamma \doteq \psi$, expressed in radians. Note that the shear strain is maximum at the neutral axis and diminishes to zero at the upper and lower surface of the beam. Shear strain causes no stretching or compression of the medium in the direction of the span. That is, the final length bb' of the element pictured in Fig. 26 is equal to its initial length aa', and similarly throughout the cross section.

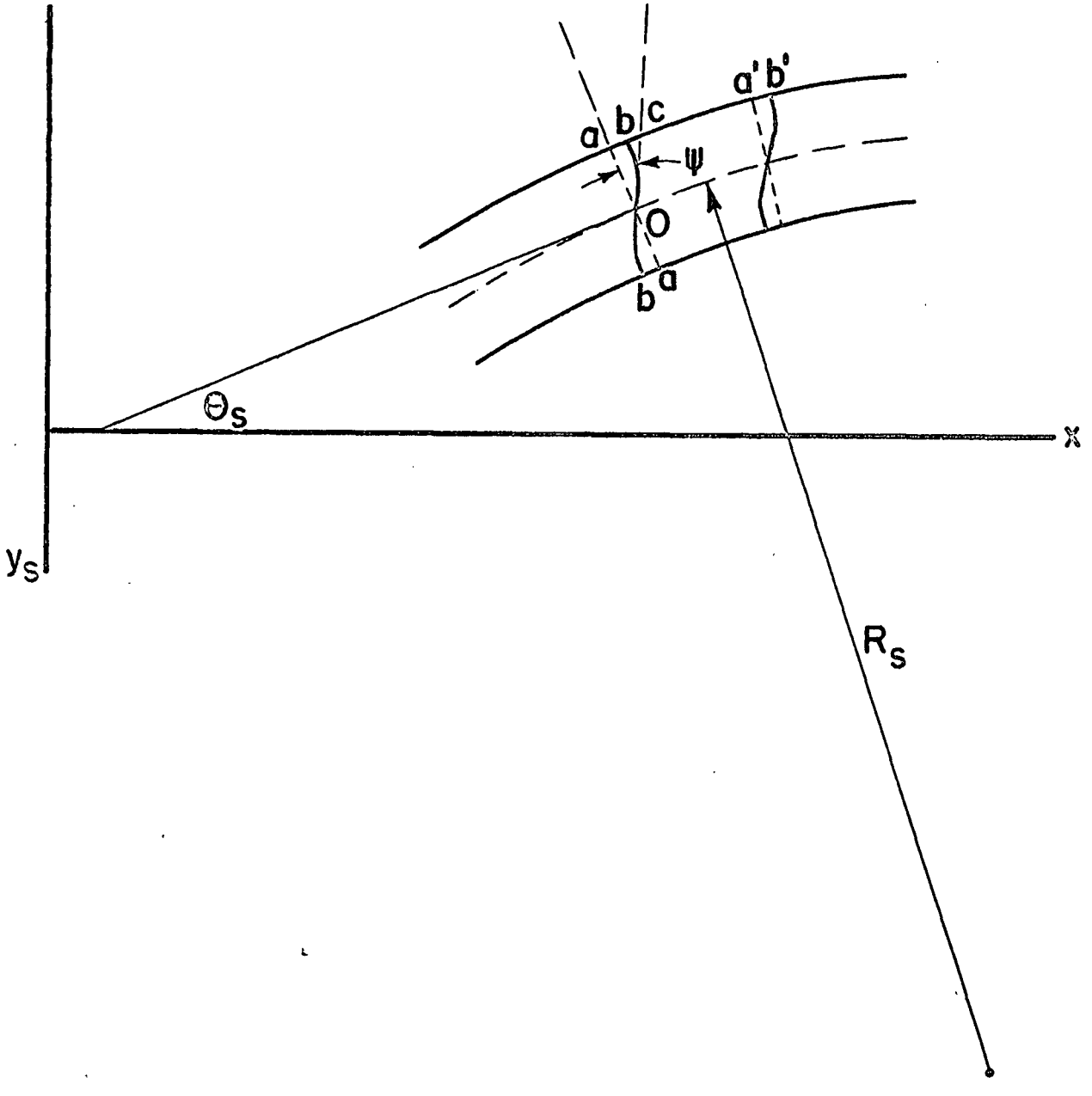

Figure 26. Deflection of Medium Due to Shear During Flute Formation

As discussed in Reference (21), the tangent line to the deflection curve (due to shear) makes an angle θ_s with the horizontal, which is numerically equal to the shear angle, ψ, at the centerline, i.e., $\theta_s = \psi$. The curvature, $1/R_s$, due to shear, therefore, is

$$\frac{1}{R_s} = \frac{d\theta_s}{ds} = \frac{d\psi}{ds} \tag{8}$$

(In the case of small deflections, $ds \doteq dx$ and $1/R_s = d\psi/dx = d\gamma/dx$, i.e., $d^2y_s/dx^2 = d\gamma/dx$.)

Using the method of superposition, the total deflection, total angle of the tangent line, and total curvature are given by

$$\begin{aligned} y_t &= y_b + y_s \\ \theta_t &= \theta_b + \theta_s \\ \frac{1}{R_t} &= \frac{1}{R_b} + \frac{1}{R_s} \end{aligned} \tag{9}$$

where the subscript t denotes the total deflected shape of the beam. In view of the equivalence of θ_s and ψ, the second of these equations becomes

$$\theta_b + \psi = \theta_t. \tag{10}$$

By means of Equations (7) and (8), the third of these equations may be written as

$$\frac{2\epsilon}{t} + \frac{d\psi}{ds} = \frac{1}{R_t} \tag{11}$$

which states that the total curvature of the beam is the sum of a term involving the maximum bending strain, ϵ, and the rate of change of shear angle, $\frac{d\psi}{ds}$. Note that if the shear angle ψ is constant over a portion of the beam (i.e., its rate of change is zero), then shear strain does not contribute to the curvature of the beam. Under these conditions, however, the shear strain will contribute to the slope of the deflected beam, according to Equation (10).

It should be recognized at this point that the basic theory presented above is in the nature of a first (and probably crude) approximation to the bending and shear strains induced during forming of a flute. The analysis is essentially that used in "engineering strength of materials." As such it reflects the assumptions and engineering experience associated with relatively stiff structures undergoing very small deflections. That is, with the exception of the experessions for curvature, the above theory is essentially a small deflection analysis. Flute forming, on the other hand, is undoubtedly in the realm of large deflection behavior. Some of the questionable assumptions and techniques employed in the analysis (questionable with respect to flute molding) are itemized below:

1. Infinitesimal vs. finite strains. The analysis assumes very small strains, while flute molding probably involves finite strains. In doubt, therefore, are (a) method of superposition of bending curvature and shear curvature; (b) distribution of shear strains across the caliper; (c) distribution of bending strains across the caliper (although the assumption employed here is appropriate for strains beyond the elastic limit); (d) no reduction in caliper (or, equivalently, absence of compressive stresses in the caliper direction).

2. Neutral surface at the mid-plane. If the tension modulus of the medium is greater than the compression modulus, the neutral surface will be displaced toward the tension side of the beam. Then the tension strain will be less than $t/2R_b$, while the compressive strain will be greater. The actual distance from the neutral surface to the beam surface should be substituted in place of $t/2$ in this expression.

3. Lateral load. Unlike a "conventional" beam, the flute is subjected to frictional forces along one surface, rather than solely lateral forces. The frictional forces may be expected to alter the distribution of shear strains across the caliper from that pictured in the beam of Fig. 26 which is shear-free at both surfaces.

4. Homogeneous material. The engineering strength of materials approach applied in this analysis has been developed for materials which are macroscopically homogeneous in their composition. It has not been rigorously established whether the methods are appropriate to fibrous materials which possess a lesser degree of homogeneity than, say, metals and plastics.

In spite of the formidability of these possible shortcomings of the theory, it is believed that it will be instructive to pursue a numerical analysis of flute forming. Although the magnitudes of the results may have questionable significance, it is felt that illustration of the principles involved and the trends developed will be helpful to an understanding of the mechanics of flute ing.

To this end, Fig. 27 shows an assumed deflected form of the medium as it passes over one tooth tip, beginning at the mid-point of one side wall and ending at the mid-point of the successive side wall. The first of the six graphs is the deflected shape of the medium centerline. The deflection co-ordinate y_t is taken as positive downward so that the curvature will be positive, for convenience. The horizontal axis is distance s along the deflected beam ($s = 0$ at the mid-point of the left-hand side wall). The side wall, of length s_w, is assumed to be straight in this approximation,

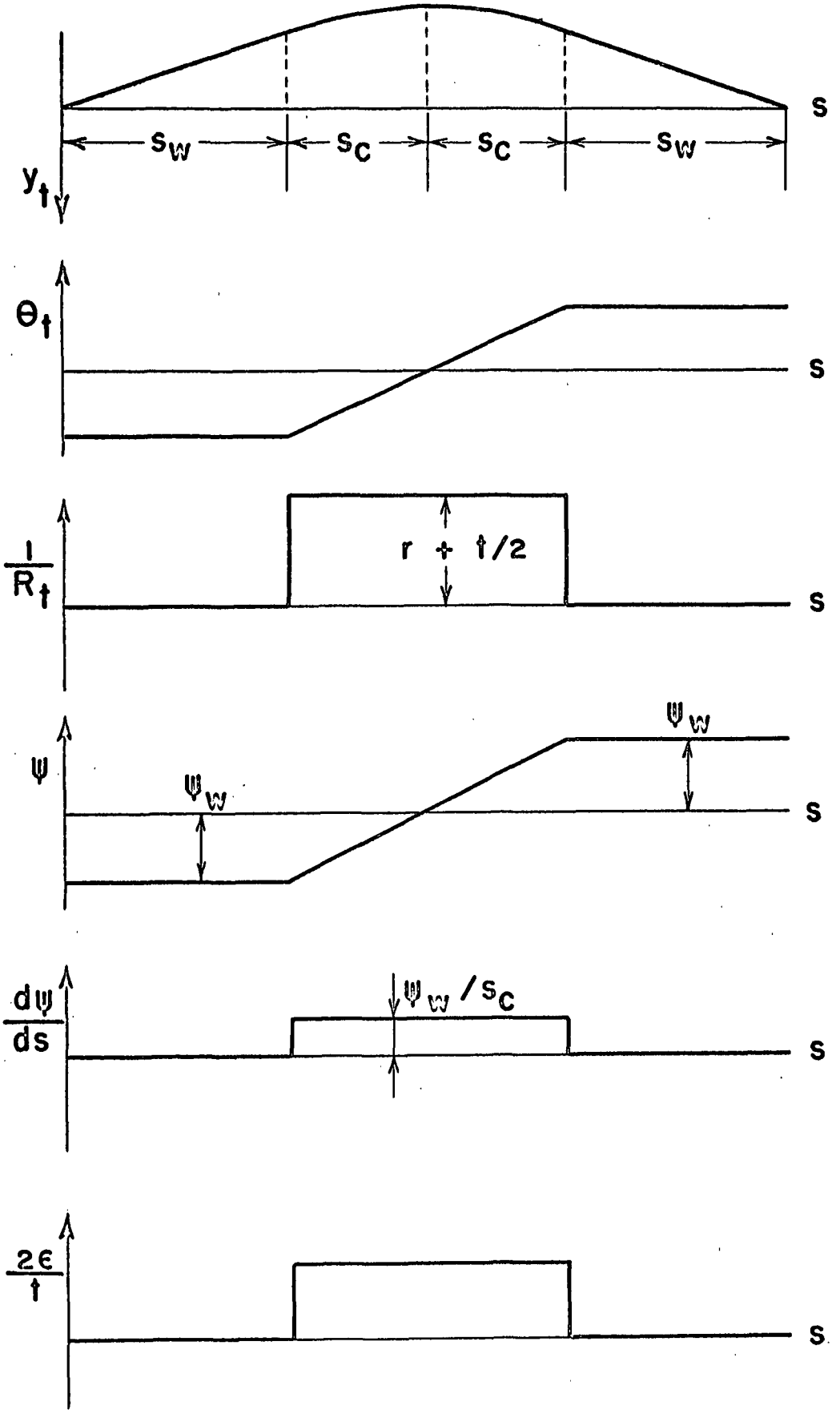

Figure 27. Assumed Deflected Shape and Distribution of Bending and Shear Strains in Fluted Medium

although in the actual flute one might expect a small amount of bending and/or shear curvature over the side wall. The succeeding portion of the deflection curve, of length 2 s_c is the part of the flute which is in contact with the tooth tip. This portion of the curve is an arc of a circle of radius $R_c = r + t/2$, where r is the radius of the tooth tip and t is the caliper of the medium. The third portion of the curve is the right-hand side wall, again a straight line by assumption.

The second and third graphs are the angle of the tangent line, θ_t, and the curvature of the flute, $1/R_t$, respectively.

The final three graphs of Fig. 27 are assumed distributions for shear angle, φ, rate of change of shear angle, $d\varphi/ds$, and bending strain, ϵ. Shear strain is taken as negative over the first side wall. By symmetry, the shear strain is necessarily zero at the center of the tooth tip ($s = s_w + s_c$). Hence, the rate of change of shear strain is positive over the tip, so that this sign convention satisfies Equation (8). The maximum value of the shear angle, without regard to sign, will be denotedby φ_w; it is assumed constant over the side wall.

The rate of change of shear strain, $d\varphi/ds$, is zero on the side walls and equal to φ_w/s_c over the tooth tip. Thus, the curvature of the flute due to shear strain is simply φ_w/s_c.

The assumed bending strain is given by the final graph of Fig. 27. The parameter $2\epsilon/t$, which is the curvature due to bending by Equation (7), is plotted rather than ϵ. Since caliper t is assumed to be constant, the ordinates to this curve are proportional to bending strain.

In view of Equation (11), the sum of the ordinates of the $\underline{d\psi/ds}$ curve and the $2\epsilon/\underline{t}$ curve is the ordinate of the $1/\underline{R_t}$ curve. That is, the sum of the shear curvature and the bending curvature is the total curvature. Over the tip of the tooth the total curvature is necessarily constant and equal to $\underline{r} + \underline{t}/2$. Thus, by Equation (11), on the flute tip the shear and bending strains are related by

$$\frac{2\epsilon}{\underline{t}} + \frac{\varphi_w}{\underline{s_c}} = \frac{1}{\underline{r} + \underline{t}/2} \qquad (12)$$

For regular A-flute, the tip radius is $\underline{r} = 0.0582$ in. Measurements made of the labyrinth drawings employed in the friction analysis gave $\underline{s_c} = 0.0725$ in. for the length of medium in contact with the tip of the last tooth prior to the center of the labyrinth. This tooth precedes nip compression of the medium and thus is expected to be the point of most severe bending and shear strain. Taking the medium caliper as $\underline{t} = 0.010$ in., Equation (12) becomes

$$\frac{2\epsilon}{0.010} + \frac{\varphi_w}{0.0725} = \frac{1}{0.0582 + 0.010/2} \qquad (13)$$

or

$$200\epsilon + 13.8\,\varphi_w = 15.82 \qquad (14)$$

Equation (14) is a relationship between bending and shear strains which will accomplish the forming of a flute, according to the assumed distributions of these strains shown in Fig. 27. A graph of this relationship is presented in the main body of this report pertaining to forming strains (Fig. 22). As pointed out in that discussion, each point on the curve gives a combination of shear and bending strains which will satisfy the forming requirements. This

analysis does not select which combination may be expected to exist for a given medium. That will depend on the material properties of the medium in shear and bending, of which this analysis takes no account.

It may be of interest to note that for the A-flute example considered here, the angle θ_b of the tangent line (due to bending) at the point where the medium enters onto the tooth tip is given by

$$\theta_b = \frac{s_c}{R_b} = (0.0725)(8.0) = 0.58 \text{ radian}$$

when $\epsilon = 0.04$ in./in. For this value of bending strains, Fig. 22 shows that the angle of the tangent due to shear is $\theta_s = \psi_w = 0.57$ radian. The total angle θ_t is

$$\theta_t = \theta_b + \theta_s = 0.58 + 0.57 = 1.15 \text{ radian} = 66°.$$

θ_t is the angle of the side wall with the horizontal and agrees with measurements made on the labyrinth drawing for the tooth under consideration.

For regular B-flute, the tip radius is $r = 0.0490$ in. and the length of medium on the tip was found to be $s_c = 0.0514$ in. With medium caliper $t = 0.010$ in., Equation (12) becomes

$$200\epsilon + 19.5 \cdot \psi_w = 18.52 \qquad (15)$$

A graph of this relationship is also given in Fig. 22.